



UNIVERSITY OF LEEDS

This is a repository copy of *Highly Productive Oxidative Biocatalysis in Continuous Flow by Enhancing the Aqueous Equilibrium Solubility of Oxygen*.

White Rose Research Online URL for this paper:
<http://eprints.whiterose.ac.uk/130668/>

Version: Supplemental Material

Article:

Chapman, MR, Cosgrove, SC, Turner, NJ et al. (2 more authors) (2018) Highly Productive Oxidative Biocatalysis in Continuous Flow by Enhancing the Aqueous Equilibrium Solubility of Oxygen. *Angewandte Chemie - International Edition*, 57 (33). pp. 10535-10539. ISSN 1433-7851

<https://doi.org/10.1002/anie.201803675>

© 2018 WILEY-VCH Verlag GmbH & Co. KGaA, Weinheim. This is the peer reviewed version of the following article: Chapman, M. ., Cosgrove, S. ., Turner, N. ., Kapur, N. and Blacker, A. J. (2018), Highly Productive Oxidative Biocatalysis in Continuous-Flow by Surpassing the Aqueous Equilibrium Solubility of Oxygen. *Angew. Chem. Int. Ed.* doi:10.1002/anie.201803675, which has been published in final form at <https://doi.org/10.1002/anie.201803675>. This article may be used for non-commercial purposes in accordance with Wiley Terms and Conditions for Self-Archiving. Uploaded in accordance with the publisher's self-archiving policy.

Reuse

Items deposited in White Rose Research Online are protected by copyright, with all rights reserved unless indicated otherwise. They may be downloaded and/or printed for private study, or other acts as permitted by national copyright laws. The publisher or other rights holders may allow further reproduction and re-use of the full text version. This is indicated by the licence information on the White Rose Research Online record for the item.

Takedown

If you consider content in White Rose Research Online to be in breach of UK law, please notify us by emailing eprints@whiterose.ac.uk including the URL of the record and the reason for the withdrawal request.



eprints@whiterose.ac.uk
<https://eprints.whiterose.ac.uk/>

SUPPORTING INFORMATION

Table of Contents

1. Materials and Methods	1
1.1 Preparation of biocatalysts	2
2. Oxygen Mass Transfer Considerations	3
2.1. Conventional laboratory batch bioreactors	3
2.2. H ₂ O ₂ /catalase fed-batch bioreactors	4
2.3. Flow gas-liquid mass transfer measurements	5
2.4. Flow Liquid-Liquid in situ O ₂ Generation Measurements	6
3. Batch Control Experiments	7
3.1. Biocatalytic reaction using aerated headspace	7
3.2. Biocatalytic reaction using air-sparged reactor	7
3.3. Biocatalytic reaction using H ₂ O ₂ source (single addition)	8
3.4. Biocatalytic reaction using H ₂ O ₂ source (fed-batch addition)	8
4. Optimisation of Flow Conditions	10
4.1. General procedure using single cascade CSTR	10
4.2. Effect of sequential H ₂ O ₂ dosing	11
4.3. General procedure using multi-point injection reactor (MPIR)	12
4.4. General procedure for conversion of 30 mM alcohol substrates (1a-1p)	13
4.5. General procedure for conversion of THIQ substrate (3a)	14
4.6. Reaction configuration	16
5. Calculation of Relative Maximal Catalyst Velocity in Flow	17
6. Reactor Design	19
6.1 Computational fluid dynamic (CFD) simulations	20
7. Gas and Liquid Chromatography Calibration Curves	22
8. Gas and Liquid Chromatography Data	25
9. HPLC Columns, Conditions and Retention Times	35
9.1. HPLC sampling	35
10. GC Columns, Conditions and Retention Times	36
11. References	37

1. Materials and Methods

Unless otherwise stated, all chemicals reported in the manuscript were obtained from Sigma-Aldrich, Fisher Scientific, Alfa Aesar or Fluorochem Ltd. and were used without further purification. Catalase (lyophilized powder) with an activity of 2000-5000 U mg^{-1} protein (one unit (U) corresponds to an amount of enzyme which decomposes 1 μmol H_2O_2 per minute at pH 7.0 and 25 $^\circ\text{C}$) and horseradish peroxidase (HRP) with an activity of 50-150 U mg^{-1} (Type I) (one unit corresponds with the amount of enzyme that forms 1 mg purpurogallin from pyrogallin in 20 seconds at pH 6.0 and 20 $^\circ\text{C}$) were acquired from Sigma-Aldrich. Galactose oxidase M_{3,5} from *Fusarium* as cell-free extract (CFE), and monoamine oxidases D5 and D9 from *Aspergillus niger* as whole-cells, were obtained from Prozymix (Haltwhistle, United Kingdom) and deployed in these forms. Solutions were made using deionized water and fresh enzyme solutions were made every day. All reaction solvents employed were of HPLC grade. Deuterated CDCl_3 was used as supplied. ^1H and ^{13}C NMR spectra were recorded on either a Bruker DPX300 (300/75 MHz) spectrometer or a Bruker AV3-400 (400/100 MHz) spectrometer using the residual solvent as an internal standard. The values of chemical shifts are reported in parts per million (ppm) with the multiplicities of the spectra reported as follows: singlet (s), doublet (d), triplet (t), quartet (q), multiplet (m) and broad (br), values for coupling constants (J) are assigned in Hz. Assignment of some ^1H NMR spectra was aided by the use of 2D ^1H - ^1H COSY experiments and the assignment of some $^{13}\text{C}\{^1\text{H}\}$ NMR spectra was aided by $^{13}\text{C}\{^1\text{H}\}$ DEPT135 experiments. Mass spectra were collected on a Bruker Daltonics (micro TOF) instrument operating in the electrospray mode.

HPLC measurements were performed on an Agilent Technologies 1100 series system. Column: YMC-pack ODS-AM, AM303 (250 mm \times 4.6 mm \times 5 μm). Solvent gradients are tabulated in Table S8. Flow rate: 1.0 mL min^{-1} . $\lambda = 254$ nm, T = 30 $^\circ\text{C}$. GC was performed using an Agilent Technologies 7890B series GC system, 7693 injector, 7693 autosampler and 5973 mass-selective detector. The method employed a HP-1 column (30 m \times 0.32 mm \times 0.25 μm), and an oven temperature ramp of 60 \rightarrow 200 $^\circ\text{C}$ (isothermal for 1 minute at 60 $^\circ\text{C}$, followed by 10 $^\circ\text{Cmin}^{-1}$ increase to 200 $^\circ\text{C}$), isothermal for 1 minute, followed by 200 \rightarrow 300 $^\circ\text{C}$ at 50 $^\circ\text{Cmin}^{-1}$, using He carrier gas (inlet pressure = 4.76 psi).

All syringe pumps were Harvard 11, all other pumps were Jasco PU980 Intelligent HPLC pumps and were connected to the flow reactors using PTFE tubing ($1/8''$ or $1/16''$ O.D.) and flangeless male HPLC nuts ($1/8''$) with flangeless ferrules ($1/8''$). Dissolved oxygen measurements were recorded on a Mettler Toledo SevenExcellence Multiparameter with InLab[®] OptiOx digital probe.

1.1 Preparation of biocatalysts

Galactose oxidase variant M_{3.5}

GOase mutant M_{3.5} was transformed into *E. coli* BL21 cells (Invitrogen) according to the manufacturer's procedure. A single colony was selected from an overnight LB plate containing 1 μ L of kanamycin of a 30 mgmL⁻¹ stock, per mL agar, and used to inoculate 5 mL TB medium supplemented with 5 μ L kanamycin and grown overnight at 37 °C and 250 rpm. 500 μ L of the culture was used to inoculate 250 mL of autoinduction medium and supplemented with 250 μ L kanamycin in a 2L Erlenmeyer flask. The cells were grown at 26 °C and 250 rpm for 60 hours. Cells were harvested by centrifugation at 6000 rpm and 4 °C for 20 minutes, then filtered through Ministart filters (0.22 μ m, Sartorius) to afford the cell-free extract which was concentrated by freeze-drying and used as a powdered cell-free extract.

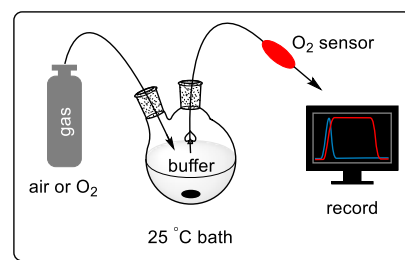
Monoamine oxidase variants D5 and D9

MAO-N mutant D9 was transformed into *E. coli* BL21 cells (Invitrogen) according to the manufacturer's procedure. A single colony was selected to inoculate a pre-culture (5 mL) which was grown in TB medium with ampicillin (100 mgL⁻¹) at 37 °C and 250 rpm, until an OD₆₀₀ between 0.6-1.0 was reached. 2L Erlenmeyer flasks containing 600 mL TB with ampicillin (100 mgL⁻¹) were inoculated with 5 mL of pre-culture and incubated at 37 °C and 250 rpm for 24 hours. Cells were harvested by centrifugation at 8000 rpm and 4 °C for 20 minutes. Cell pellets were stored at -20 °C until needed.

2. Oxygen Mass Transfer Considerations

2.1 Conventional Laboratory Batch Bioreactors

A round-bottomed flask (500 mL) was charged with Ar-purged NaPi buffer (200 mL, pH 7.4) and a magnetic stir bar (50 mm × 10 mm). The temperature and pressure of the flask was maintained constant (25 °C and 1013 mbar, respectively). The solution was stirred at 800 rpm, and the dissolved O₂ content was recorded in situ over time using a dO₂ sensor.



Gas → liquid O₂ transfer batch setup

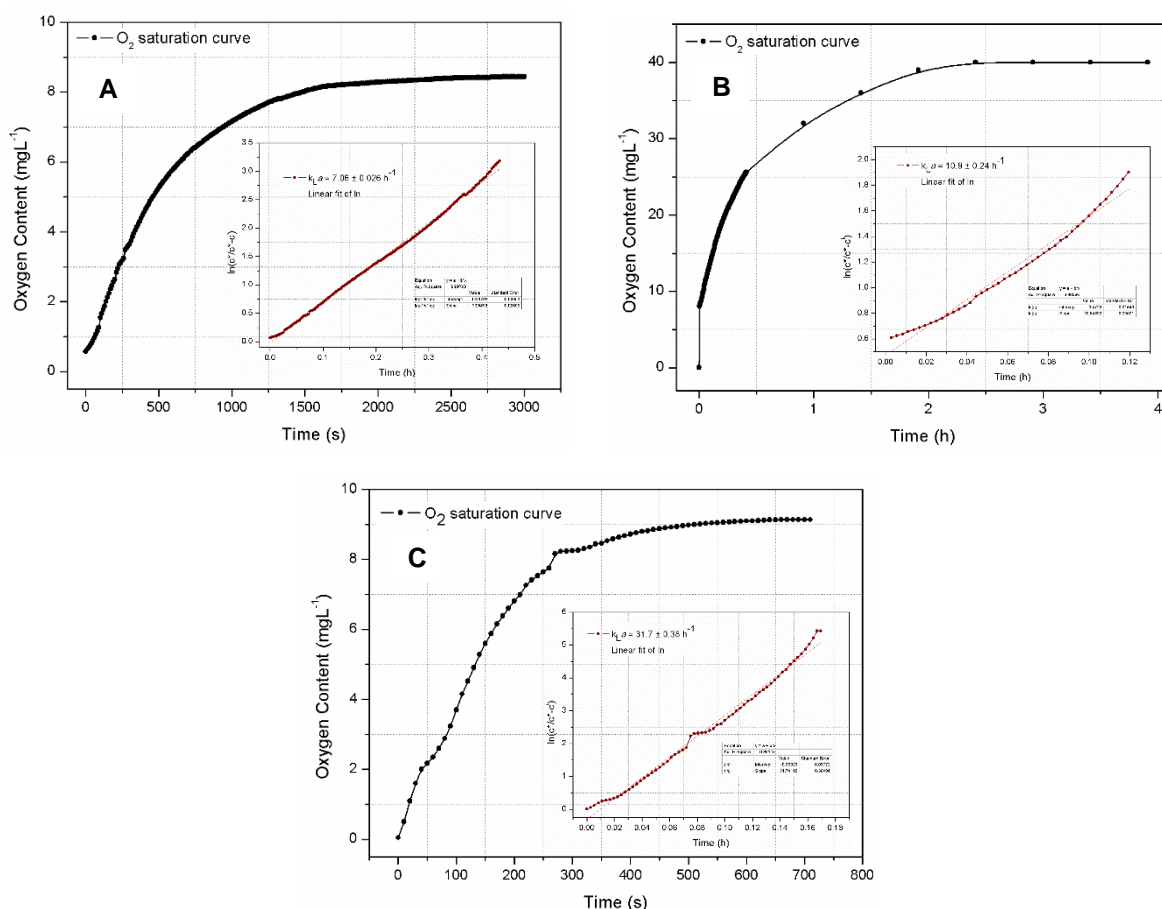


Figure S1. Oxygen saturation curves obtained in batch mode, with k_La extrapolation inset images. Conditions: **A** = aerated headspace, **B** = O₂ headspace, **C** = air-sparging (0.5 vvm). T = 25 °C, P = 1013 mbar, M = 800 rpm.

Entry	Reactor Type	c^{init}/c^{final} [mgL ⁻¹]	k_La^a [h ⁻¹]	OTR ^b [mgO ₂ L ⁻¹ h ⁻¹]
A	Air headspace	0.2/8.4	7.06 ± 0.03	60
B	O ₂ headspace	0.2/40	10.90 ± 0.24	440
C	Air sparged	0.2/9.4	31.7 ± 0.38	300

Table S1. Mass transfer data for O₂ gas → liquid in conventional batch mode. ^aMass transfer coefficients calculated from initial rate data. ^bOTR = oxygen transfer rate.

2.2 H₂O₂/Catalase Fed-Batch Bioreactor

A round-bottomed flask (500 mL) was charged with Ar-purged NaPi buffer (200 mL, pH 7.4), catalase enzyme (0.25 mgmL⁻¹, 2000-5000 Umg⁻¹), antifoam 204 (0.01 wt. %) and a magnetic stir bar (50 mm × 10 mm). The temperature and pressure of the flask was maintained constant (25 °C and 1013 mbar, respectively). A separate solution of aqueous H₂O₂ (0.18 M, excess) was fed via syringe pump into the flask at a range of flow-rates, and the mixture stirred at 800 rpm. The dissolved O₂ content was recorded in situ over time using a dO₂ sensor.

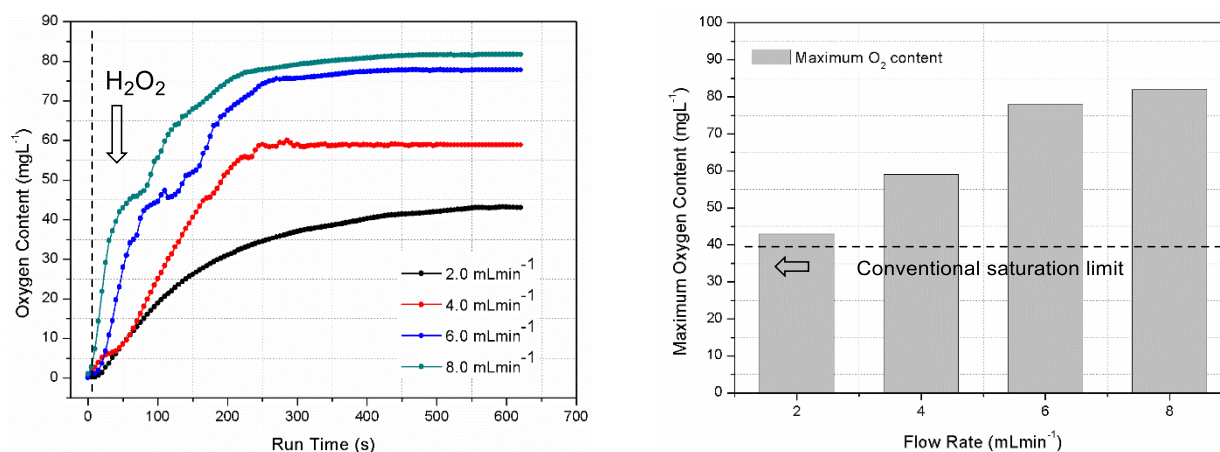
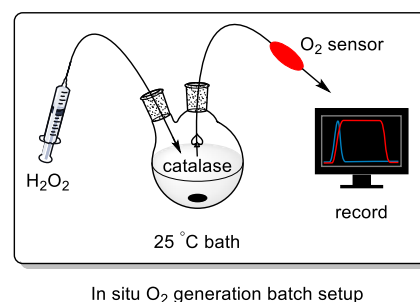


Figure S2. Oxygen saturation curves obtained in fed-batch mode, via H₂O₂ decomposition. Left: plot of [O₂] vs time, during constant addition of H₂O₂ at 2, 4, 6 and 8 mLmin⁻¹. Right: column plot of the maximum observed [O₂] at each flow-rate. T = 25 °C, P = 1013 mbar, M = 800 rpm.

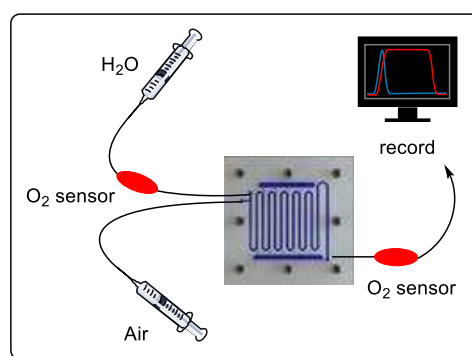
Entry	Flow-rate [mLmin ⁻¹]	Saturation limit [mgL ⁻¹]	Time to exceed 40 mgL ⁻¹ (min)	OSR ^a [mgO ₂ L ⁻¹ h ⁻¹]
1	2	43	6.6	364
2	4	59	2.5	960
3	6	78	1.25	1920
4	8	82	0.75	3200

Table S2. Oxygen supersaturation data. ^aOSR = oxygen supersaturation rate.

2.3 Flow Gas-Liquid Mass Transfer Measurements

The rate of mass transfer of gaseous oxygen from air into water was assessed using the plate bioreactor. Two gas-tight syringes were attached to the reactor inlets (reservoir inlets blocked).

Feed 1: air. Feed 2: Ar-purged demineralised H₂O (0.1 mgL⁻¹ dO₂ measured at 19 °C, 1013 mbar). Each feed was pumped through the reactor at a range of flow-rates, and the dissolved O₂ content of the eluent recorded over time. A control void of air flow into the reactor measured 0 mgL⁻¹ dO₂, with O₂-saturated H₂O recorded at 8.5 mgL⁻¹.



Gas → liquid O₂ transfer flow setup

Entry	Flow-rate ^a [mLmin ⁻¹]	τ_{res} [min]	dO ₂ ^b [mgL ⁻¹]	$k_L a^c$ [h ⁻¹]	OTR ^d [gO ₂ L ⁻¹ h ⁻¹]
1	0.17	15.0	8.30	166	1.4
2	0.26	10.0	8.33	293	2.4
3	0.52	5.0	8.29	474	3.9
4	1.3	2.0	8.26	1033	8.5
5	2.6	1.0	8.23	1900	15.6
6	5.2	0.5	7.11	609	4.3
7	10.4	0.25	4.93	331	1.6

Table S3. Mass transfer data for O₂ gas → liquid in plate bioreactor. ^aFlow-rates are combined. ^bMeasured at ambient temperature (19 °C) and steady-state. ^c c_{sat} observed = 8.5 mgL⁻¹. ^dOTR = oxygen transfer rate.

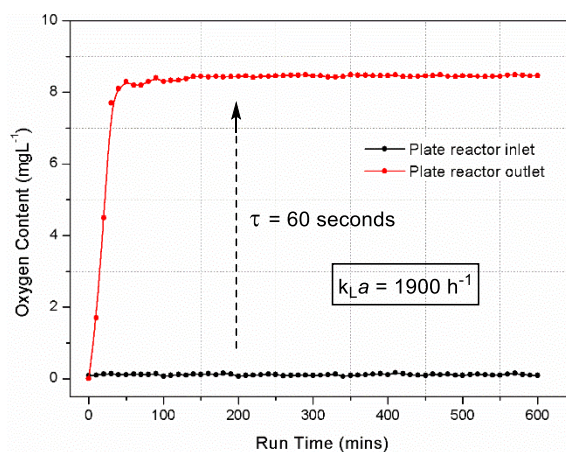


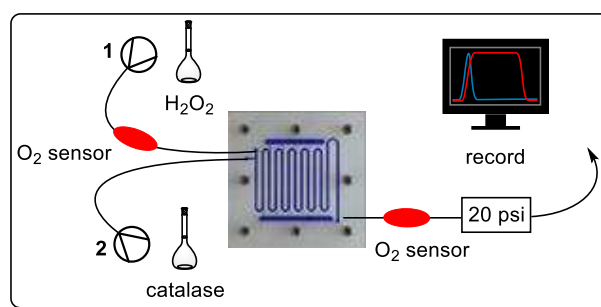
Figure S3. Steady-state oxygen concentration plot, measured at inlet/outlet of plate reactor (conditions taken from entry 5 of Table S3).

2.4 Flow Liquid-Liquid in situ O₂ Generation Measurements

The quantity of in situ generated dissolved oxygen was measured using the plate bioreactor. Two pumps were attached to the reactor inlets (reservoir inlets blocked). The reactor outlet was linked to a low-threshold back-pressure regulator (20 psi), purely to facilitate control over volumetric flow-rate.

Feed 1: Ar-purged NaPi buffer (pH 7.4) (0.1 mgL⁻¹ dO₂ measured at 19 °C, 1013 mbar), containing H₂O₂ (variable concentration) and antifoam 204 (0.01 wt. %).

Feed 2: analogous solvent, containing catalase enzyme (catalase enzyme (0.25 mgmL⁻¹, 2000-5000 Umg⁻¹). Each feed was pumped through the reactor at a range of flow-rates, and the dissolved O₂ content of the eluent recorded over time. A control void of air flow into the reactor measured 0 mgL⁻¹ dO₂, with O₂-saturated H₂O recorded at 8.5 mgL⁻¹.



Liquid → liquid O₂ generation flow setup

Entry	[H ₂ O ₂] [mM]	Flow-rate ^a [mLmin ⁻¹]	τ_{res} [min]	dO ₂ ^b [mgL ⁻¹]	Supersaturation ^c [%]
1	50	0.13	20	71	78
2	100	0.13	20	99	148
3	150	0.13	20	121	203
4	200	0.13	20	140	250
5	250	0.13	20	151	278
6	300	0.13	20	155	288
7	300	0.26	10	152	280
8	300	0.52	5	144	260

Table S4. In situ O₂ generation data in plate bioreactor. ^aFlow-rates are combined. ^bMeasured at ambient temperature (19 °C) and steady-state. ^cCalculated at steady-state, as [(recorded [O₂] - 40 mgL⁻¹)/40 mgL⁻¹].

3. Batch Control Experiments

3.1 Biocatalytic reaction using aerated headspace (modified from Woodley and Turner)^[1]

A biooxidation reaction was conducted in a 500 mL round-bottomed flask equipped with magnetic stir bar (200 mL reaction volume). The flask was charged with aqueous NaPi buffer (200 mL, 100 mM, pH 7.4), benzyl alcohol (650 mg, 6.0 mmol), GOase M_{3.5} (100 mg, 0.5 mgmL⁻¹ CFE), HRP type I (38 mg, 10 UmL⁻¹), catalase (12.5 mg, 125 UmL⁻¹), CuSO₄ (1.6 mg, 50 μM) and stirred at room temperature (800 rpm). Samples were withdrawn at regular time intervals and analysed by HPLC.

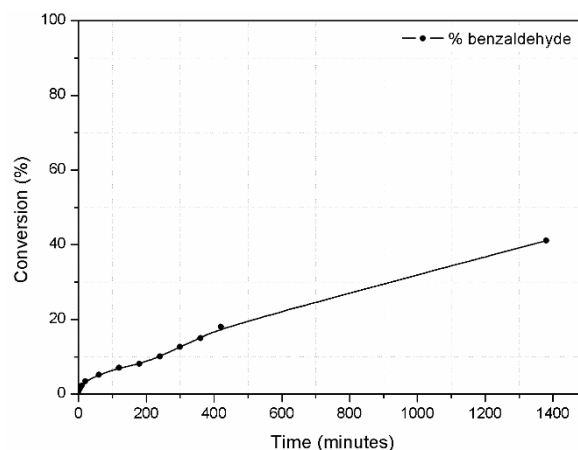


Figure S4. Conversion vs time profile for the bio-oxidation of benzyl alcohol, using an aerated batch vessel.

3.2 Biocatalytic reaction using air-sparged reactor

An analogous procedure to that described above was performed, with 0.5 vvm air-sparging. Note: volatile product was stripped with off-gas, resulting in an incomplete mass balance.

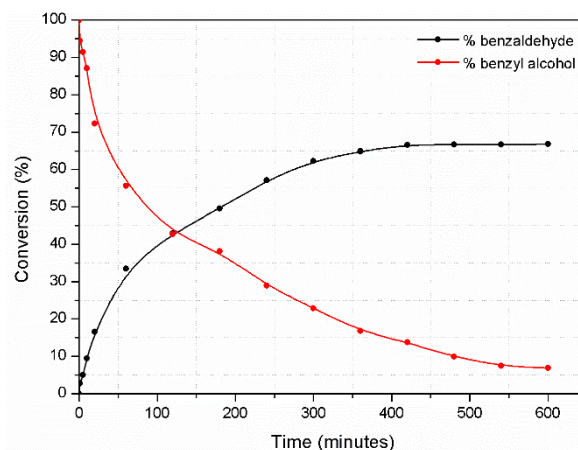


Figure S5. Conversion vs time profile for the bio-oxidation of benzyl alcohol, using an air-sparged batch vessel.

3.3 Biocatalytic reaction using H₂O₂ source (single addition)

A biooxidation reaction was conducted in a 500 mL round-bottomed flask equipped with magnetic stir bar (200 mL reaction volume). The flask was charged with aqueous NaPi buffer (200 mL, 100 mM, pH 7.4), benzyl alcohol (650 mg, 6.0 mmol), GOase M₃₋₅ (100 mg, 0.5 mgmL⁻¹ CFE), HRP type I (38 mg, 10 UmL⁻¹), catalase (12.5 mg, 125 UmL⁻¹), CuSO₄ (1.6 mg, 50 μM) and stirred at room temperature (800 rpm). A single portion of H₂O₂ (0.7 mL of 30 % ν /_v in 19.3 mL buffer, 1 equiv.) was added to the flask, upon which vigorous gas evolution was observed (O₂ generation) for the first 15 – 20 minutes. Samples were withdrawn at regular time intervals and analysed by HPLC, with the dissolved O₂ content monitored by a dO₂ sensor.

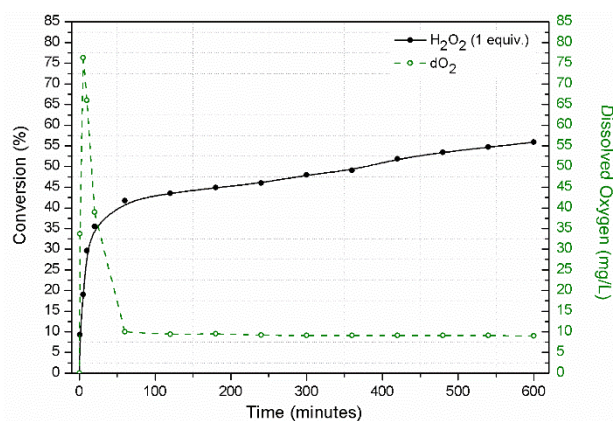


Figure S6. Conversion vs time profile for the bio-oxidation of benzyl alcohol, whilst applying an external source of H₂O₂ in a single portion.

3.4 Biocatalytic reaction using H₂O₂ source (fed-batch addition)

An analogous batch reaction was configured to that described above. A solution of H₂O₂ (1.4 mL of 30 % ν /_v in 28.6 mL buffer, 2 equiv., [or double]) was added to the flask via syringe pump (0.2 mLmin⁻¹, 150 minutes), during which steady gas evolution was observed (O₂ generation). Throughout and following, the mixture was stirred at 800 rpm at room temperature. Samples were withdrawn at regular time intervals and analysed by HPLC, with the dissolved O₂ content monitored by a dO₂ sensor.

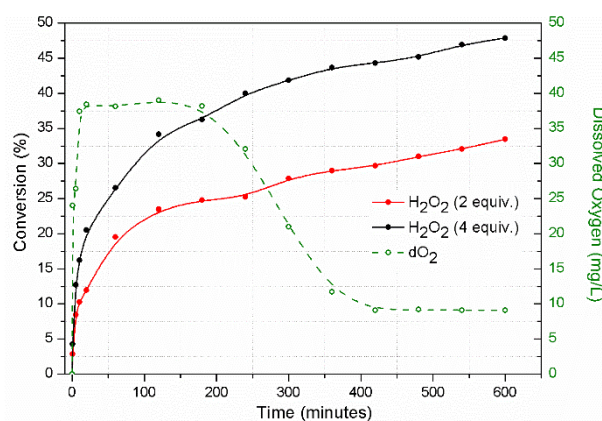


Figure S7. Conversion vs time profiles for the bio-oxidation of benzyl alcohol, whilst applying an external source of H₂O₂ as a slow feed (right).

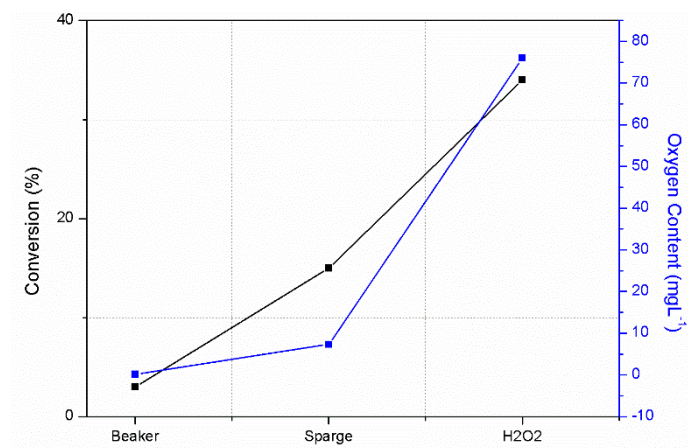
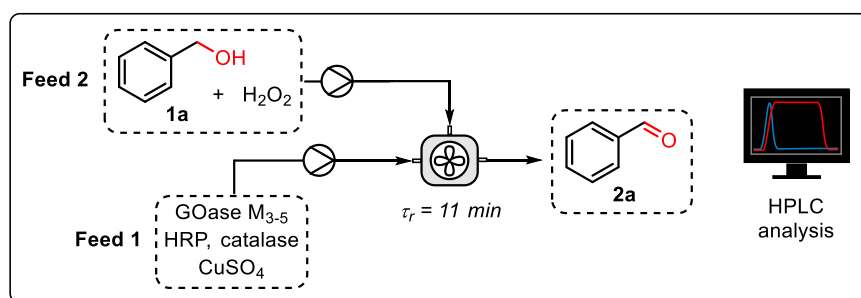


Figure S8. Comparison plot between observed conversion and O₂ content, for 3 different batch bio-oxidation modes. Each point is taken 20 minutes into the respective reaction (beaker, sparge and H₂O₂ single addition).

4. Optimisation of Flow Conditions

4.1 General procedure using single cascade CSTR



Experimental configuration for initial optimisation of biooxidation

A biooxidation reaction was conducted in a single-stage CSTR, linked to two liquid pumps.

Feed 1: GOase M₃₋₅ (variable), HRP type I (0.1 mgmL⁻¹), catalase (variable) and CuSO₄ (0.125 mgmL⁻¹), dissolved in NaPi buffer (pH 7.4).

Feed 2: benzyl alcohol (30 mM) and H₂O₂ (variable) dissolved in uniform solvent.

Note: control experiments indicated each mixture was stable for at least 5 days with no sign of decomposition, stored at 4 °C.

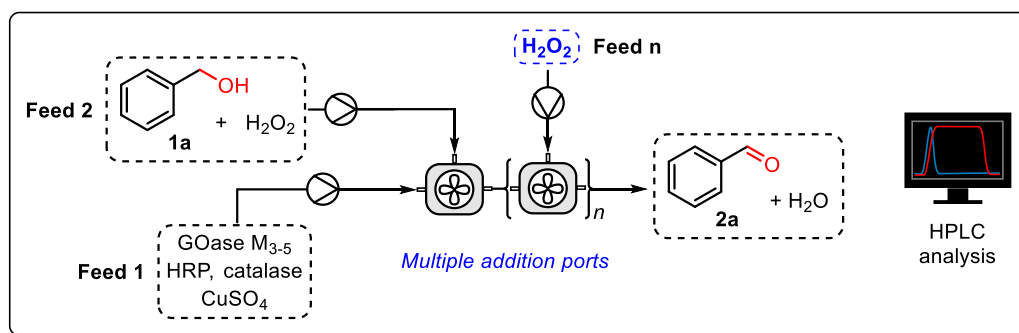
Each solution was pumped continuously at 0.09 mLmin⁻¹ (τ_r = 11 minutes) and stirred at 1100 rpm at room temperature. Samples were collected from the eluent at regular time intervals and analysed by HPLC.

Entry	[GOase] [mgmL ⁻¹]	[H ₂ O ₂] [mM]	[Catalase] [mgmL ⁻¹]	Conversion [%] ^a
1	0.5	30	0.1	2
2	0.5	60	0.1	5
3	0.5	120	0.1	9
4	0.5	240	0.1	11
5	1.0	120	0.1	19
6	1.0	240	0.1	21
7	4.0	120	0.1	33
8	4.0	240	0.1	33
9	6.5	120	0.1	40
10	6.5	240	0.1	41
11 ^b	6.5	240	0.1	43
12	6.5	240	0.2	42
13	6.5	0	0.2	< 1

Table S5. Initial reaction optimisation study of GOase biooxidation in single CSTR. ^aDetermined by HPLC analysis under steady-state conditions. ^bResidence time doubled.

Note: where H₂O₂/catalase loading are highest, foam formation becomes problematic if no antifoam agent is used.

4.2 Effect of sequential H₂O₂ dosing



A biooxidation reaction was conducted in a multi-stage CSTR, with chamber 1 linked to two liquid pumps and subsequent chambers in-series connected to independent H₂O₂ feeds.

Feed 1: GOase M₃₋₅ (6.5 mgmL⁻¹, CFE), HRP type I (0.1 mgmL⁻¹), catalase (0.13 mgmL⁻¹) and CuSO₄ (0.125 mgmL⁻¹), dissolved in NaPi buffer (pH 7.4).

Feed 2: benzyl alcohol (30 mM), H₂O₂ (variable) and antifoam 204 (0.01 wt. %) dissolved in uniform solvent.

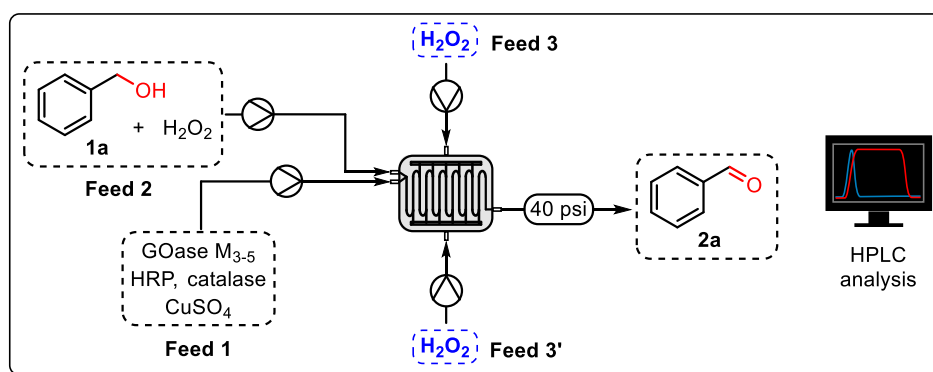
Feed n: H₂O₂ (variable) and antifoam 204 (0.01 wt. %) dissolved in uniform solvent.

Feeds 1 and 2 were pumped continuously into chamber 1 at 0.1 mLmin⁻¹, whilst the remaining equivalents of H₂O₂ were pumped via feed n across n chambers in series to achieve the residence times indicated below, each stirred at 1100 rpm at room temperature. Samples were collected from the eluent at regular time intervals and analysed by HPLC.

Entry	[H ₂ O ₂] [mM]	No. CSTRs (n)	τ _r (min)	Conversion [%] ^a
1	120	2	11	64
2	120	2	22	67
3	240	2	11	74
4	300	3	13	84
5	300	4	13	90
6	300	4	26	95
7 ^b	300	4	13	92
8	0	4	26	18

Table S6. Effect of sequential addition of H₂O₂ across reactor geometry. ^aDetermined by HPLC analysis under steady-state conditions. ^bGOase and substrate loading doubled.

4.3 General procedure using multi-point injection reactor (MPIR)



Initial reaction optimisation using MPIR

A biooxidation reaction was conducted in a multi-point injection plate reactor, with a total of four inlet feeds connected to 4 independent pumps, and a back-pressure regulator (40 psi) connected to the outlet to facilitate control over volumetric flow-rate.

Feed 1: GOase M_{3.5} (6.5 mgmL⁻¹, CFE), HRP type I (0.1 mgmL⁻¹), catalase (0.13 mgmL⁻¹) and CuSO₄ (0.125 mgmL⁻¹), dissolved in NaPi buffer (pH 7.4).

Feed 2: benzyl alcohol (30 mM), H₂O₂ (variable) and antifoam 204 (0.01 wt. %) dissolved in uniform solvent.

Feed 3: H₂O₂ (variable) and antifoam 204 (0.01 wt. %) dissolved in uniform solvent.

Feed 3': analogous to feed 3, via a separate pump.

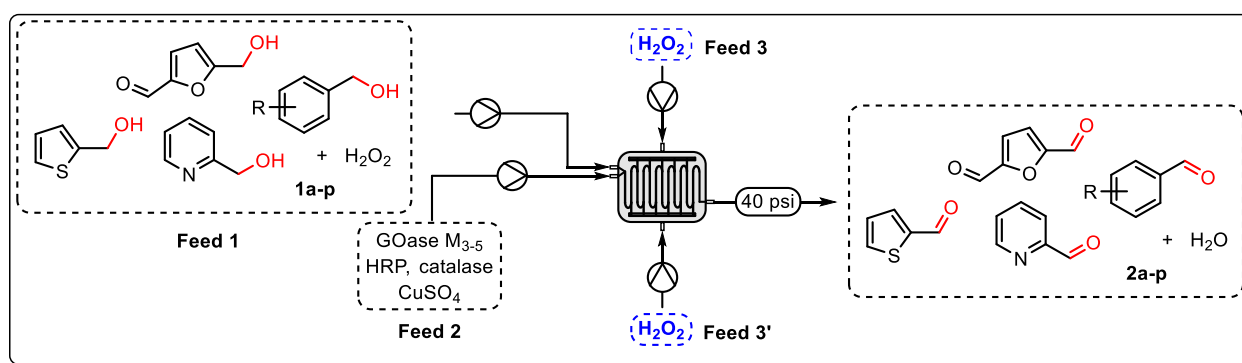
Feeds 1 and 2 were pumped continuously at equal flow-rate, whilst the remaining equivalents of H₂O₂ were pumped via feeds 3 and 3' through sub-channels into the master channel of the reactor, to achieve the residence times indicated below. Mechanical mixing occurs in the reactor via bends in the channel, with additional mixing originating from bubble formation/travel along the channel. Samples were collected from the eluent at regular time intervals and analysed by HPLC.

Entry	[Substrate] [mM]	[GOase] [mgmL ⁻¹]	[τ _{res}] [min]	H ₂ O ₂ [equiv.] ^a	Conversion [%] ^b
1	30	6.5	12	10	>99
2	30	6.5	10	10	>99
3	30	6.5	8	10	>99
4	30	6.5	8	6.6	>99
5	30	6.5	8	3.3	>99
6	30	6.5	8	1.7	84
7	30	6.5	8	3	97
8	45	6.5	8	3	88
9	60	6.5	8	3	70
10	60	6.5	8	5	79
11	60	6.5	12	10	>99

12	75	6.5	12	10	95
13	90	6.5	12	10	85
14	90	15	12	10	95
15	120	15	12	10	81
16	120	20	12	10	90
17	150	25	12	15	90
18	150	20	20	15	87

Table S7. Reaction optimization/productivity study of GOase biooxidation in MPIR. ^aEquivalents relative to substrate. ^bDetermined by HPLC analysis under steady-state conditions. Green row: optimized conditions for 30 mM substrate, carried forward. Blue row: highest productivity obtained in the MPIR.

4.4 General procedure for conversion of 30 mM alcohol substrates (1a-1p)



Substrate expansion using optimised flow conditions

A biooxidation reaction was conducted in a multi-point injection plate reactor, with a total of four inlet feeds connected to 4 independent pumps, and a back-pressure regulator (40 psi) connected to the outlet to facilitate control over volumetric flow-rate.

Feed 1: GOase M₃₋₅ (6.5 mgmL⁻¹, CFE), HRP type I (0.1 mgmL⁻¹), catalase (0.13 mgmL⁻¹) and CuSO₄ (0.125 mgmL⁻¹), dissolved in NaPi buffer (pH 7.4).

Feed 2: alcohol substrate (30 mM), H₂O₂ (1 equiv.) and antifoam 204 (0.01 wt. %) dissolved in uniform solvent. *for substrates with low solubility, additional DMSO was added to the feed to ensure homogeneity during pumping (see Table S8 below).

Feed 3: H₂O₂ (1 equiv.) and antifoam 204 (0.01 wt. %) dissolved in uniform solvent.

Feed 3': analogous to feed 3, via a separate pump.

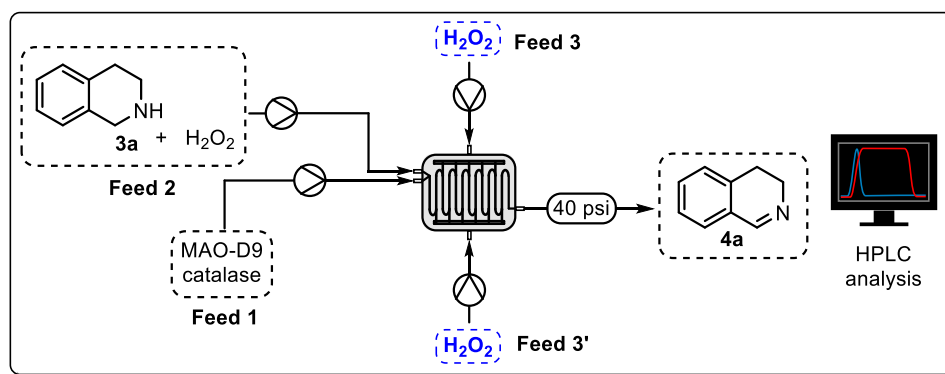
Feeds 1 and 2 were pumped continuously at equal flow-rate (80 μLmin⁻¹), whilst the remaining equivalents of H₂O₂ were pumped via feeds 3 and 3' through sub-channels into the master channel of the reactor (each at 80 μLmin⁻¹), to achieve an overall residence time of 8 minutes. Samples were collected from the eluent at regular time intervals and analysed by HPLC.

Summary of reaction solvent ratio:

Substrate	R	DMSO (v/v %) ^a
1a	H	0
1b	4-OMe	0
1c	4-CN	10
1d	4-NO ₂	20
1e	4-CF ₃	20
1f	4- ^t Bu	5
1g	3-F	0
1h	2-Cl	10
1i	4-Br	10
1j	3-I	20 ^b
1k	4-SMe	5
1l	3,5-OMe	5
1m	3-NO ₂ , 4-Cl	20
1n	Pyridyl	0
1o	Thiophenyl	0
1p	Furfural	0

Table S8. ^aRemainder of solvent is aqueous sodium phosphate buffer, pH 7.4. ^bSubstrate concentration reduced to 15 mM due to poor solubility.

4.5 General procedure for conversion of THIQ substrate (3a)



Initial reaction optimisation using MPIR

A biooxidation reaction was conducted in a multi-point injection plate reactor loaded with glass beads (2 mm dia., worth 1 mL in volume), with a total of four inlet feeds connected to 4 independent pumps, and a back-pressure regulator (40 psi) connected to the outlet to facilitate control over volumetric flow-rate.

Feed 1: MAO-D9 (80 mgmL⁻¹, whole cells) and catalase (0.13 mgmL⁻¹), dissolved in NaPi buffer (pH 7.4).

Feed 2: tetrahydroisoquinoline (10 mM), H₂O₂ (variable) and antifoam 204 (0.01 wt. %) dissolved in uniform solvent.

Feed 3: H₂O₂ (3 equiv. relative to THIQ) and antifoam 204 (0.01 wt. %) dissolved in uniform solvent.

Feed 3': analogous to feed 3, via a separate pump.

Feeds 1 and 2 were pumped continuously at equal flow-rate, whilst the remaining equivalents of H₂O₂ were pumped via feeds 3 and 3' through sub-channels into the master channel of the reactor, to achieve the residence times indicated below. Mechanical mixing occurs in the reactor via bends in the channel/tortuous flow around glass beads, with additional mixing originating from bubble formation/travel along the channel. Samples were collected from the eluent at regular time intervals and analysed by HPLC.

Entry	[Substrate] [mM]	[MAO] [mgmL ⁻¹]	[τ_{res}] [min]	H ₂ O ₂ [equiv.] ^a	Conversion [%] ^b
1 ^c	30	5	12	5	~ 3
2 ^c	20	5	12	5	~ 5
3 ^c	10	5	12	5	10
4 ^c	10	10	12	5	18
5 ^c	10	20	12	5	25
6 ^c	10	20	8	3	23
7 ^d	10	20	8	3	49
8 ^d	10	20	8	6	61
9 ^d	10	40	8	3	83
10 ^d	10	60	8	3	94
11 ^d	10	80	12	3	97
12 ^d	10	80	12	0	19

Table S9. Reaction optimisation study of MAO biooxidation in MPIR. ^aEquivalents relative to substrate.

^bDetermined by HPLC analysis under steady-state conditions. ^cWithout glass beads. ^dWith glass beads. Green row: optimised conditions for 30 mM substrate, carried forward.

4.6 Reaction configuration

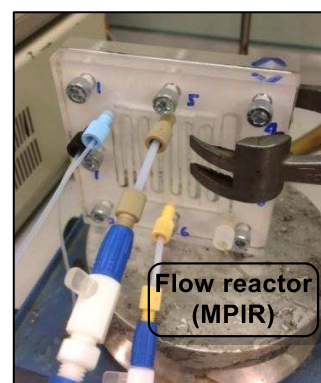
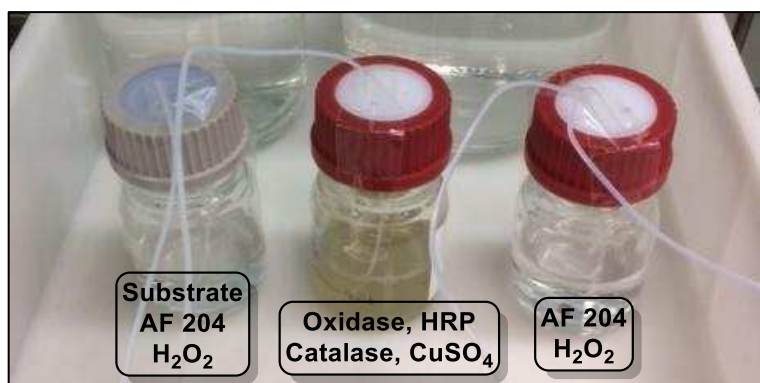
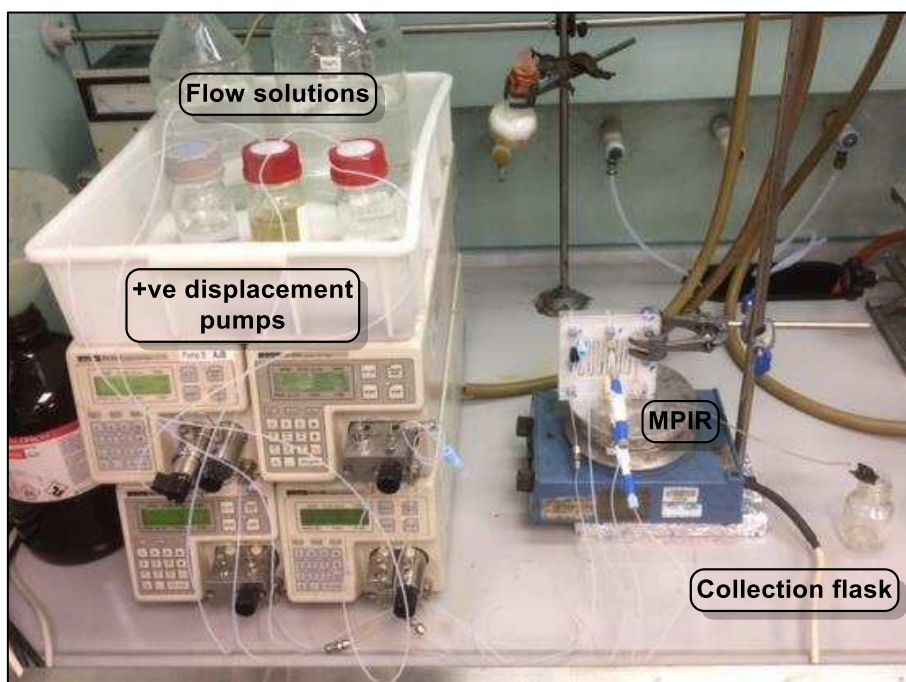


Figure S9. Images of typical continuous-flow configuration. AF = antifoam.

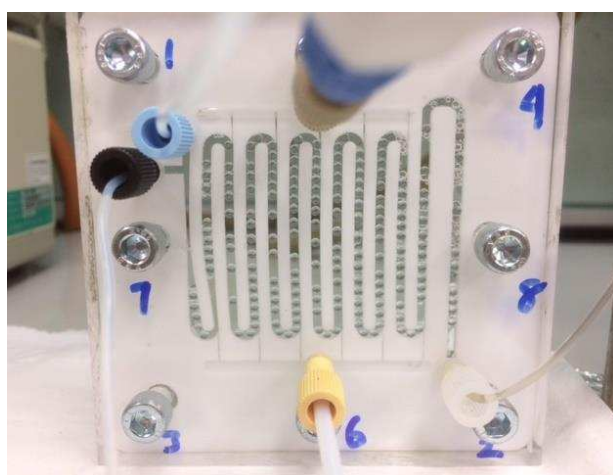


Figure S10. Image of MPIR loaded with glass beads, reducing volume by 1 mL.

5. Calculation of Relative Maximal Catalyst Velocity in Flow

5.1 Observed V_{\max} of purified GOase M₃₋₅ enzyme in batch

The activity of the cell-free extract (CFE) of GOase M₃₋₅ was found to be 3.8 μmg^{-1} under standard assay conditions, corresponding to ca. 5 % of the activity obtained when using the purified enzyme (78 μmg^{-1}). A plot of specific activity for the pure enzyme against benzyl alcohol concentration is supplied below in Figure S11.

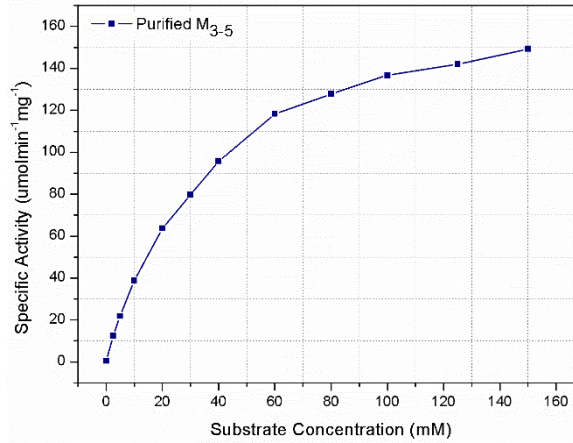


Figure S11. Specific activity of purified GOase M₃₋₅ enzyme against benzyl alcohol concentration.

Where [benzyl alcohol] = 7.5 mM, $V_{\max} = 30 \mu\text{molmin}^{-1}\text{mg}^{-1}$ of purified enzyme. As the CFE represents 5 % pure enzyme, $V_{\max} = 1.5 \mu\text{molmin}^{-1}\text{mg}^{-1}$ CFE at 7.5 mM substrate loading (common concentration in flow reactor).

5.2 Calculated V_{\max} of CFE in flow bioreactor

Expressing the rate of reaction (v) in terms of volume of substrate solution within the reactor (Vol_s) and time (t), we can derive a relative observed velocity for the enzyme based upon K_m (150 mM for benzyl alcohol)^[1] and fractional conversion (X) at steady-state (0.95 for this manuscript), where Vol_s and t are loosely considered to be reactor volume and residence time, respectively.

$$v = -\text{Vol}_s \frac{d[S]}{dt} = \frac{V_{\max}[S]}{K_m + [S]}$$

Therefore:

$$\int_0^t \frac{V_{\max}}{\text{Vol}_s} dt = - \int_{[S]_0}^{[S]} \left(1 + \frac{K_m}{[S]}\right) d[S]$$

Boundary condition: $[S] = [S]_0$ at $t = 0$:

$$\frac{V_{\max}}{\text{Vol}_s} t = ([S]_0 - [S]) - K_m \ln \left(\frac{[S]}{[S]_0} \right)$$

As fractional conversion = X :

$$X = \frac{[S]_0 - [S]}{[S]_0} \quad \equiv \quad [S]_0 - [S] = [S]_0 X$$

Substituting for:

$$\frac{V_{\max}}{\text{Vol}_s} t = [S]_0 X - K_m \ln(1 - X)$$

$$V_{\max} = \frac{([S]_0 X) - K_m \ln(1 - X) \text{Vol}_s}{t}$$

$$V_{\max} = \frac{((7.5) \times (0.95)) - (150 \cdot \ln(1 - 0.95) \cdot 0.0026)}{8} = 10^3 \mu\text{molmin}^{-1}$$

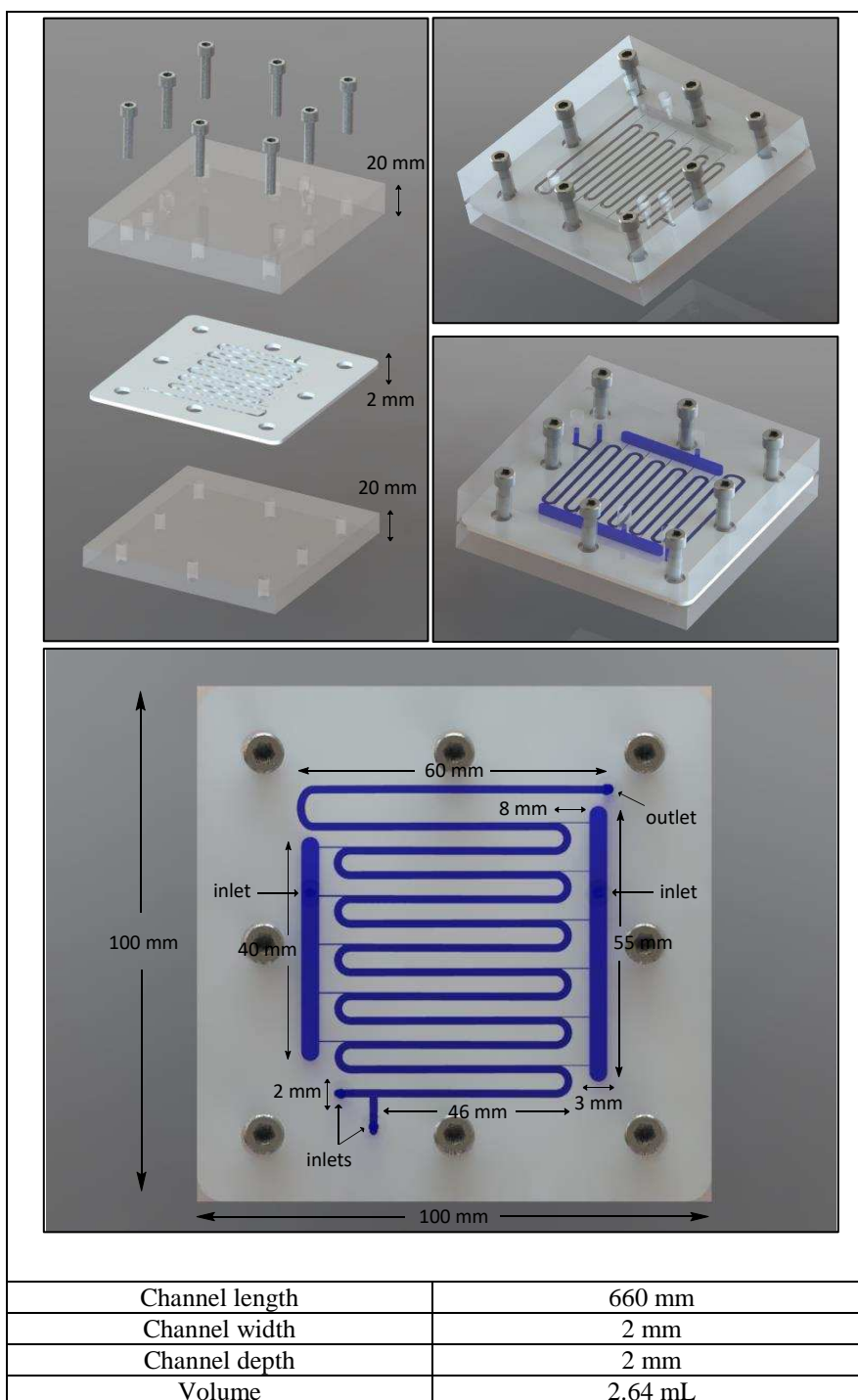
Concentration of CFE = $6.5 \text{ mgmL}^{-1} \times 2.6 \text{ mL} = 17 \text{ mg CFE per RV}$.

$$10^3/17 = \underline{59 \mu\text{molmin}^{-1}\text{mg}^{-1} \text{CFE}}$$

As an approximation, the CFE used in the flow protocol operates at ca. 40-fold higher velocity than the maximal velocity obtained under standard assay conditions. It is noteworthy, however, that the assay is performed under and relies solely upon atmospheric air to rejuvenate the biocatalyst (i.e. a mass transfer limited regime), where the continuous-flow methodology is not placed under this restriction. For this reason, the calculated velocities are only relative numbers and are not ideally comparable.

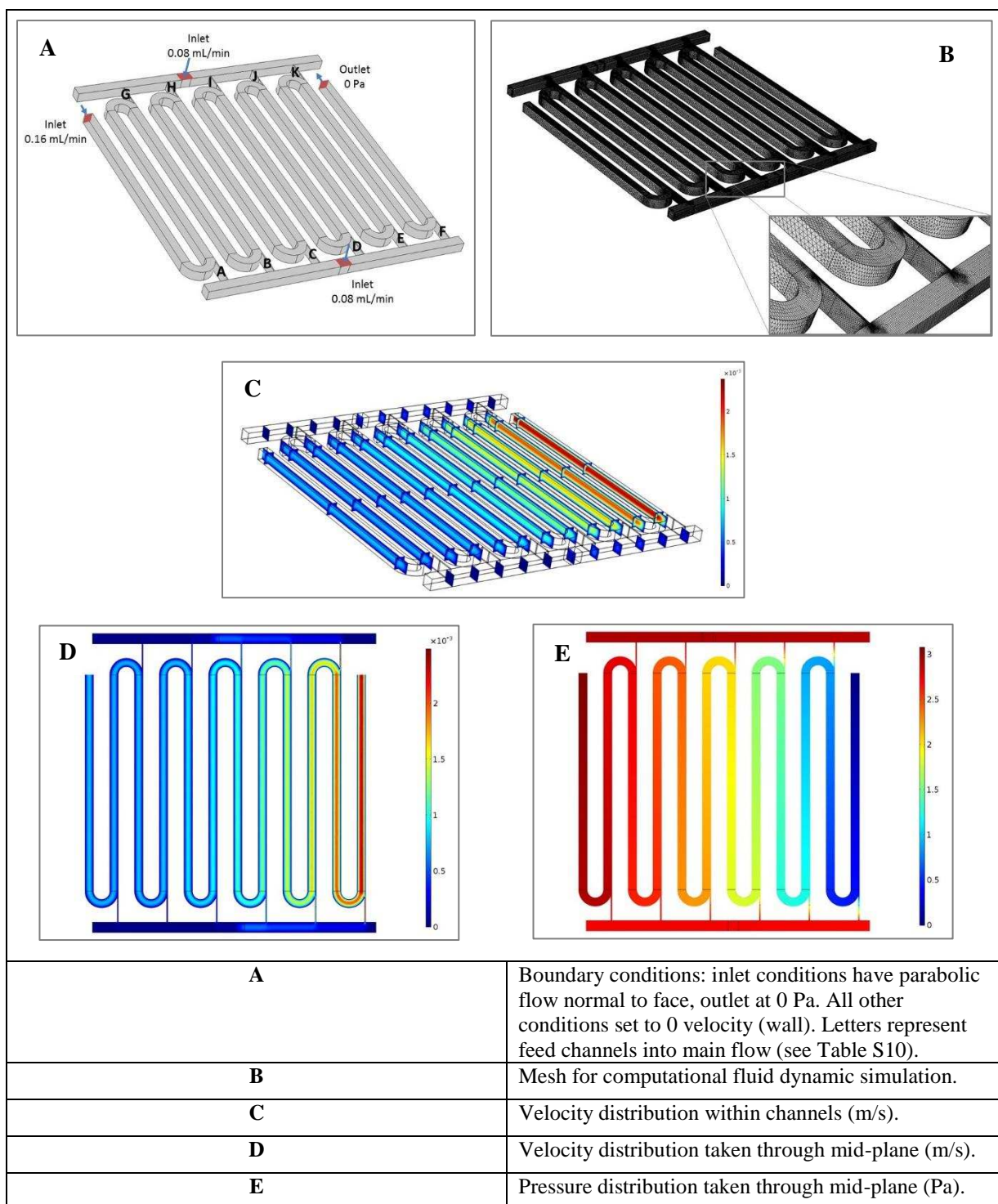
6. Reactor Design

A simple continuous-flow bioreactor was constructed by encasing a Teflon gasket between two Perspex blocks. The Teflon spacer houses a winding flow-channel which has been cut via laser, to the specification implemented using the software package ‘CorelDraw, 2016’. A pair of grooves are etched into the front Perspex block, which align perpendicular to a series of 11 laser-thin (0.1 mm) microchannels built into the Teflon spacer design. Two inlets, alongside two reservoir inlets and one outlet port were manufactured by a hand-drill and hand-tapped to create threaded sections for standard HPLC fixtures and fittings to connect. Eight peripheral bolts are used to seal the reactor upon assembly (see below for simulated reactor design images).



6.1 Computational fluid dynamic (CFD) simulations

Computational fluid dynamics were used to simulate and assess the velocity and pressure distributions in the MPIR. Variation is seen between the flow-rates of H₂O₂ micro-feeds (Table S10 for the flow conditions simulated in 6.1A). The pressure within the feed channels is largely constant, but each port enters the main channel at a different location; the decrease in pressure within the main channel as the exit is approached therefore gives an increasing flow. It would be possible to balance the flow-rate by modifying the width and/or length of entry ports, but for simplicity in the first instance these have been kept constant.

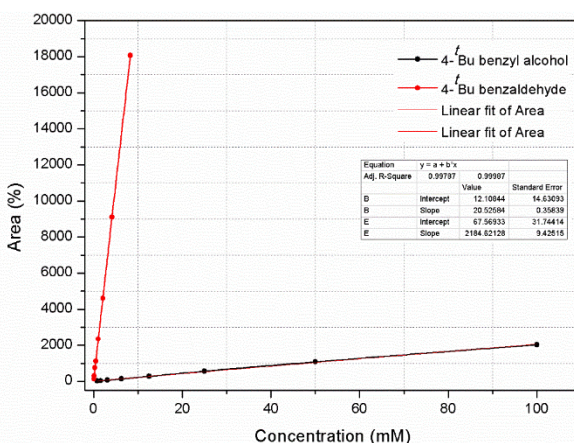
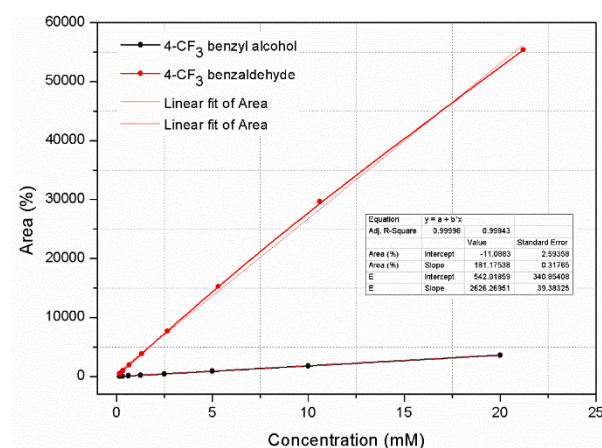
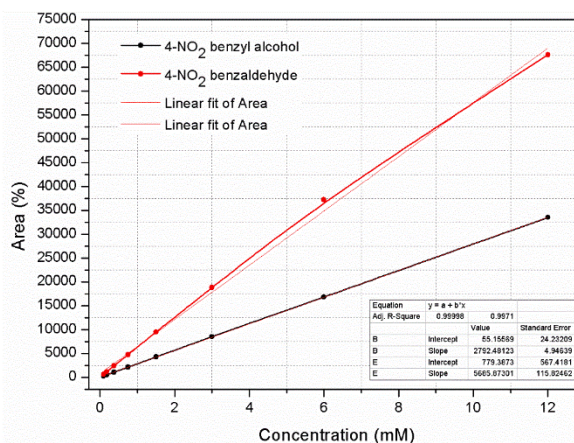
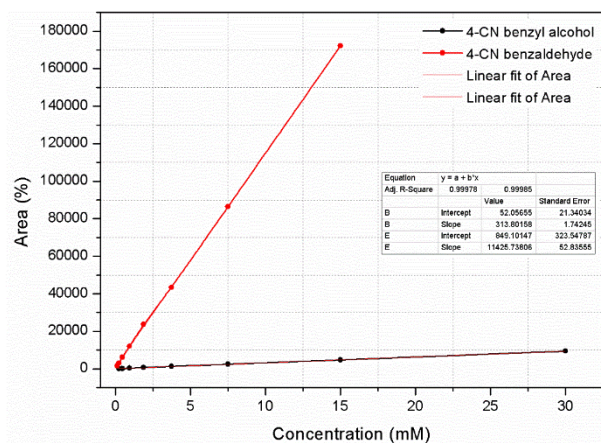
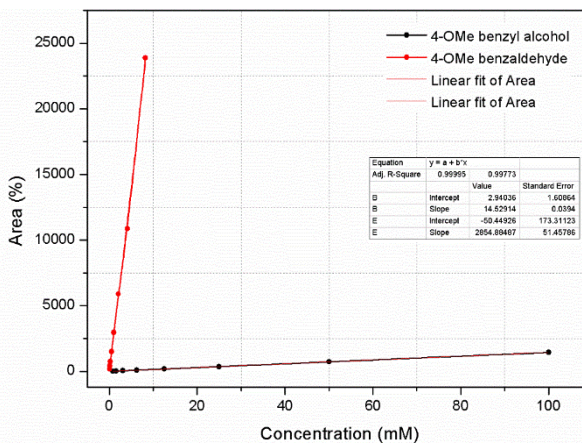
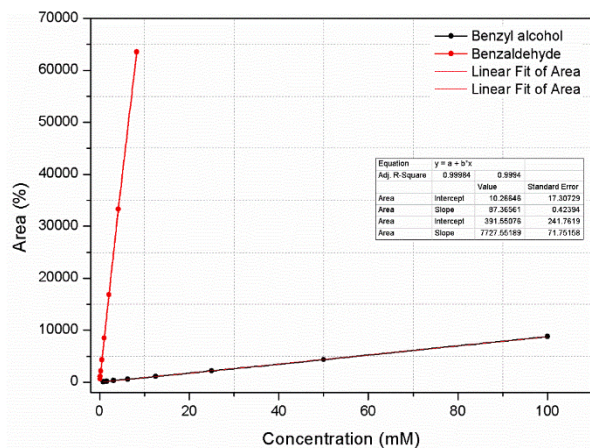


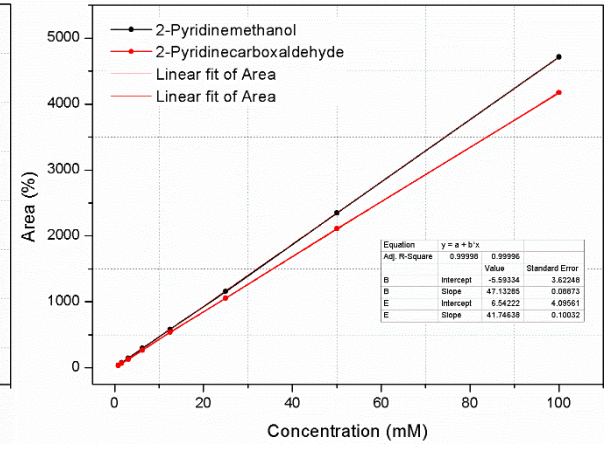
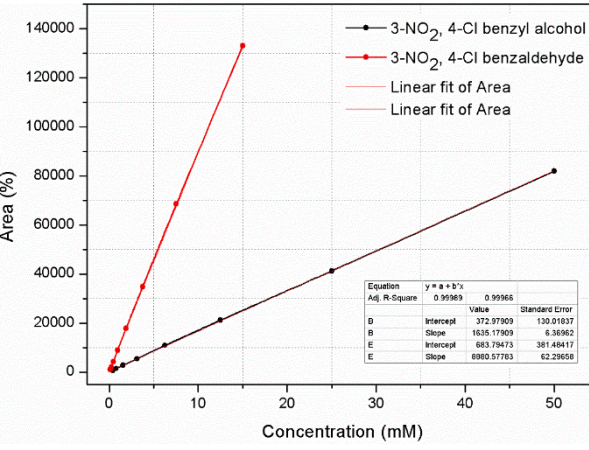
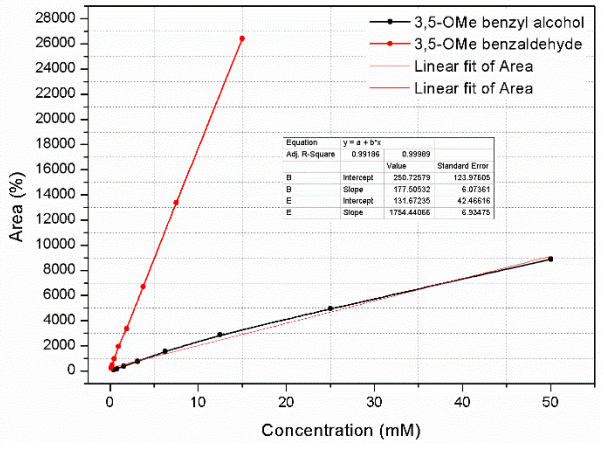
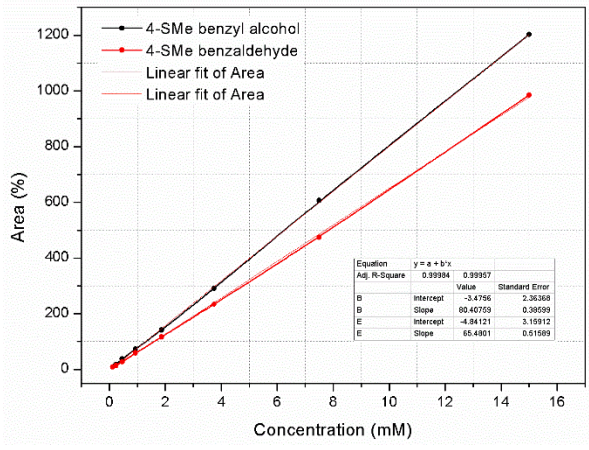
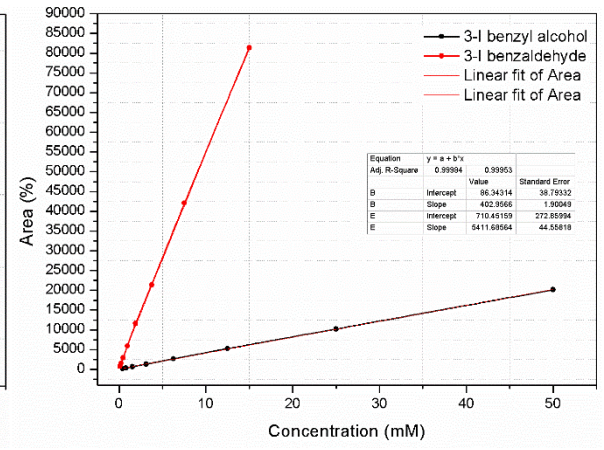
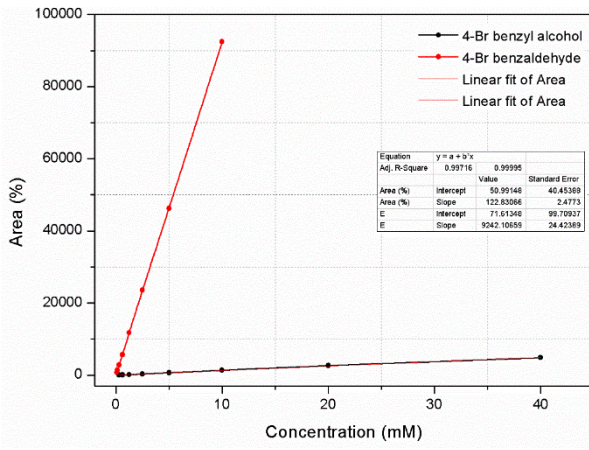
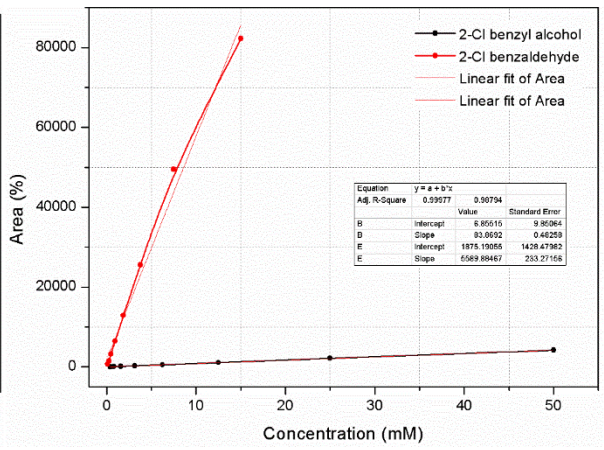
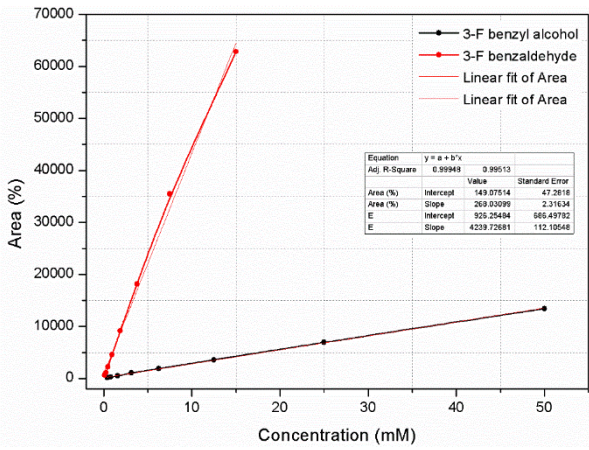
Port	mL/min
A	0.0028
B	0.0019
C	0.0071
D	0.0132
E	0.0212
F	0.0323
G	0.0027
H	0.0076
I	0.0131
J	0.0200
K	0.0295

Table S10. Variation in flow-rate between micro-channel H₂O₂ feeds, simulated by CFD.

7. Gas and Liquid Chromatography Calibration Curves

Calibration. Calibration curves with an internal standard were created for quantitative GC and HPLC analysis of reaction products. The identity of the products was additionally confirmed by GC/HPLC co-injection of reaction mixtures with chemically synthesized authentic products, or by NMR spectroscopic analysis of products obtained from reactions performed on preparative scale.





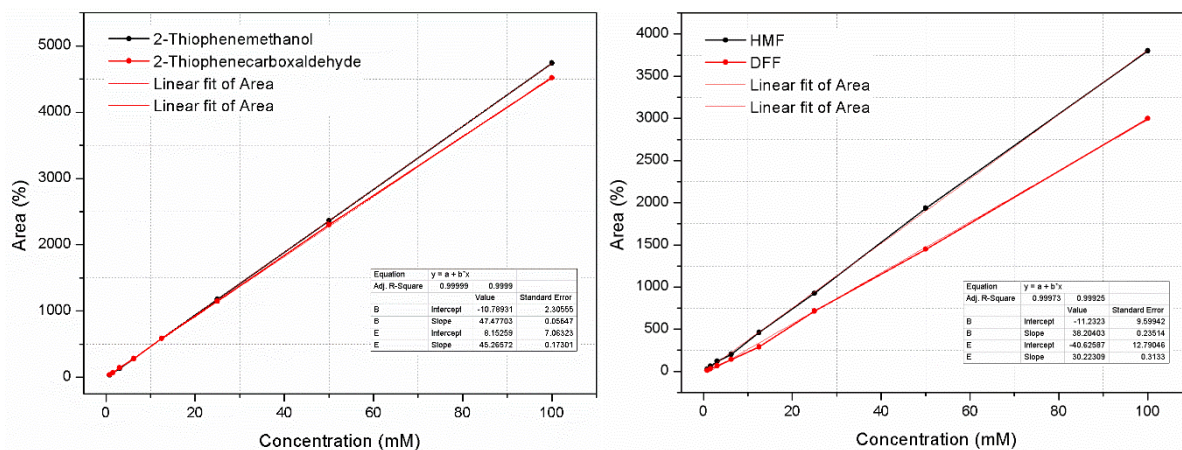


Figure S12. HPLC calibration profiles of authentic alcohol substrates (**1a-p**) and aldehyde products (**2a-p**).

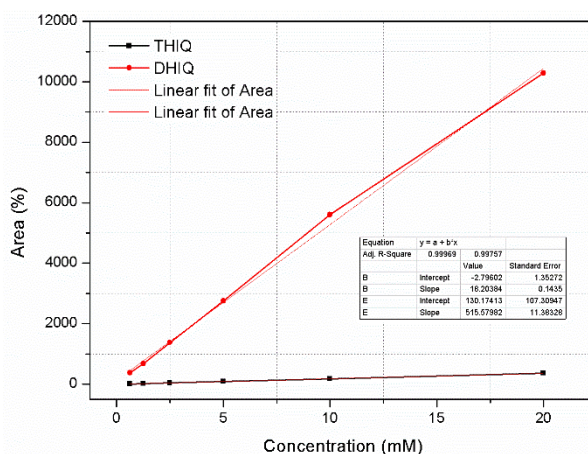


Figure S13. HPLC calibration profile of authentic THIQ substrate (**3a**) and DHIQ product (**4a**).

8. Gas and Liquid Chromatography Data

Note: peaks observed at ~ 3.3 minutes are attributable to UV-active components of Antifoam 204, with those at ~ 12.5 minutes corroborate with 1,3,5-trimethoxybenzene as internal standard.

Benzaldehyde, 2a:

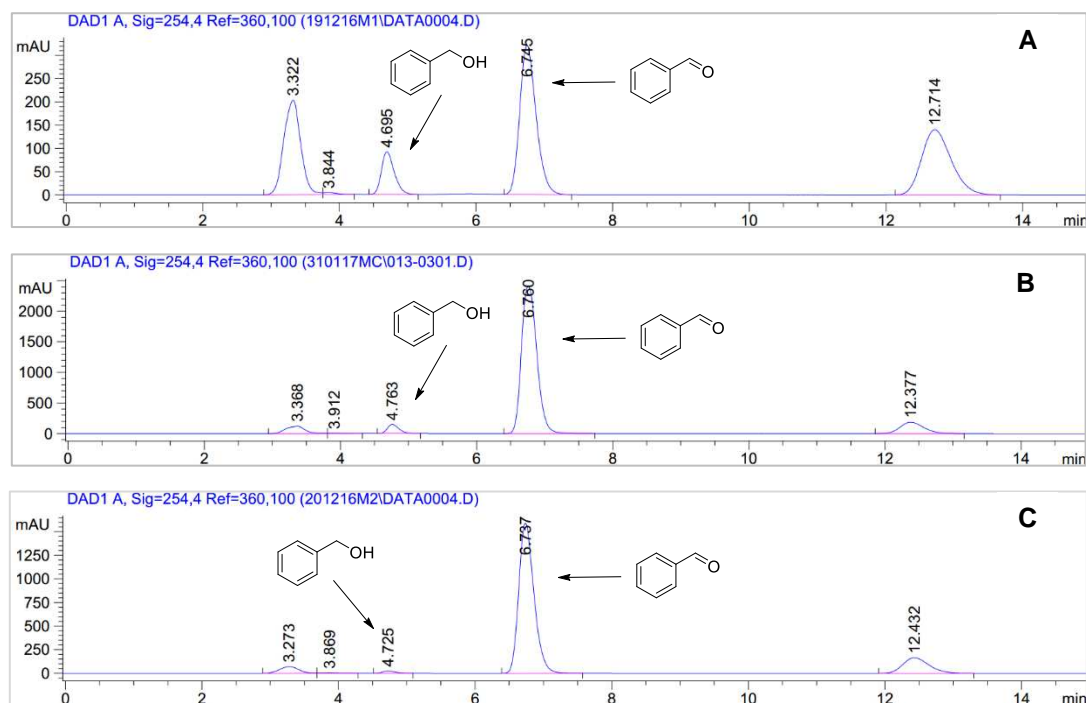


Figure S14. HPLC traces of continuous-flow oxidation of benzyl alcohol, using GOase M₃₋₅ biocatalyst. Traces indicate solution composition after 1 RV (A), 3 RVs (B) and at steady-state (C).

4-Methoxybenzaldehyde, 2b:

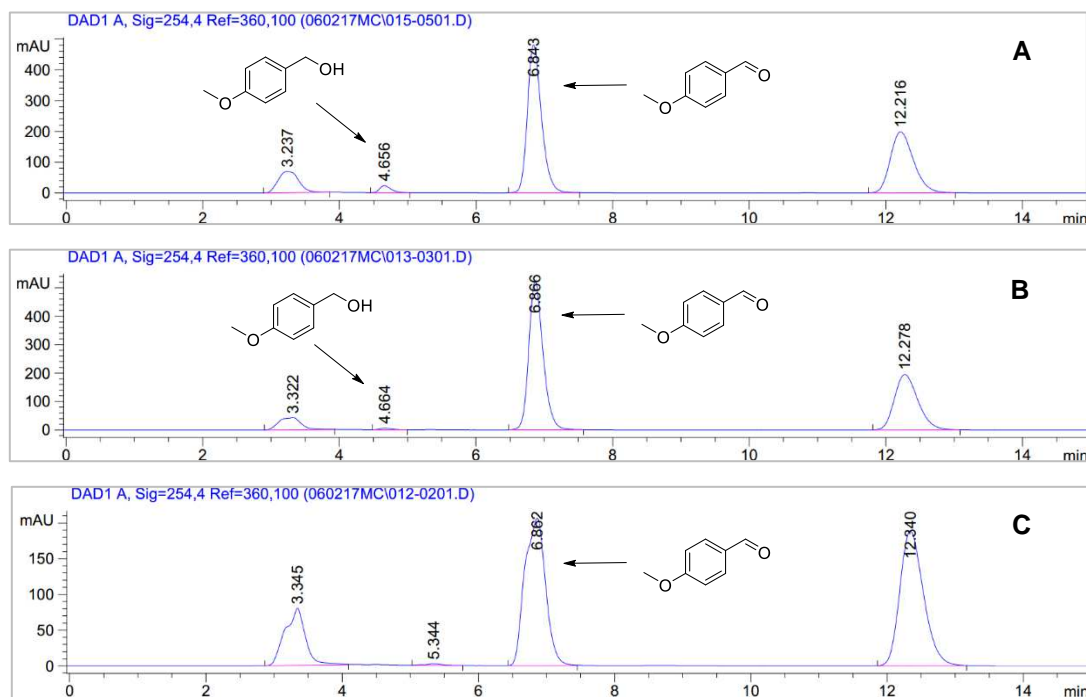


Figure S15. HPLC traces of continuous-flow oxidation of 4-methoxybenzyl alcohol, using GOase M₃₋₅ biocatalyst. Traces indicate solution composition after 1 RV (A), 3 RVs (B) and at steady-state (C).

4-Cyanobenzaldehyde, 2c:

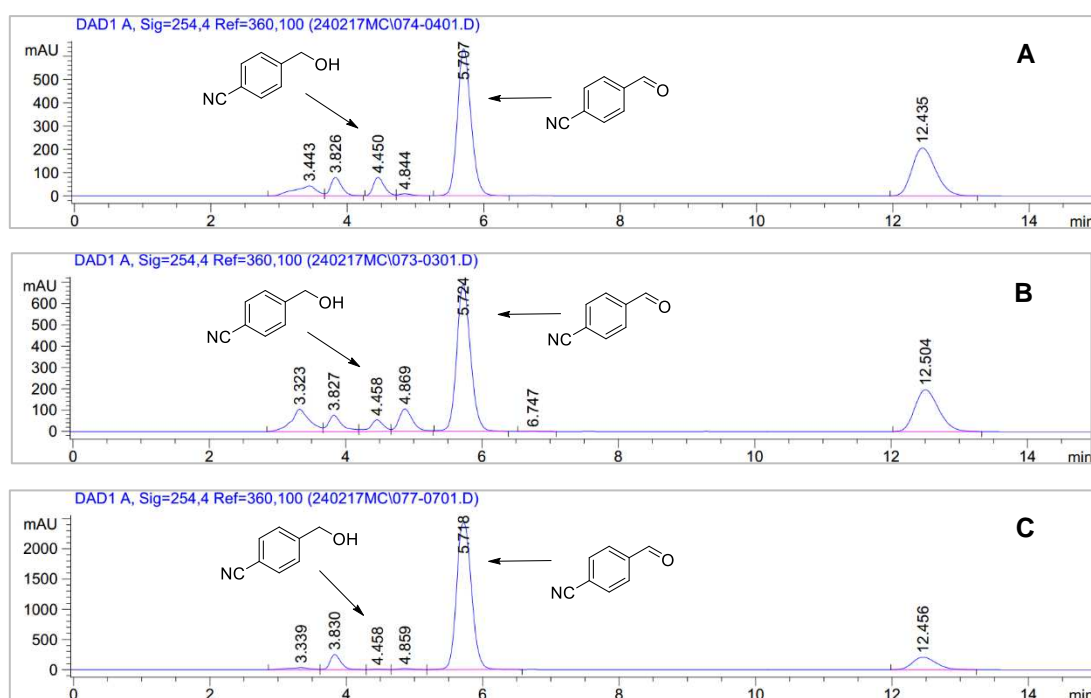


Figure S16. HPLC traces of continuous-flow oxidation of 4-cyanobenzyl alcohol, using GOase M₃₋₅ biocatalyst. Traces indicate solution composition after 1 RV (**A**), 3 RVs (**B**) and at steady-state (**C**). Peak observed at ~ 4.8 minutes attributable to a UV-active substance derived from commercially obtained 4-cyanobenzyl alcohol.

4-Nitrobenzaldehyde, 2d:

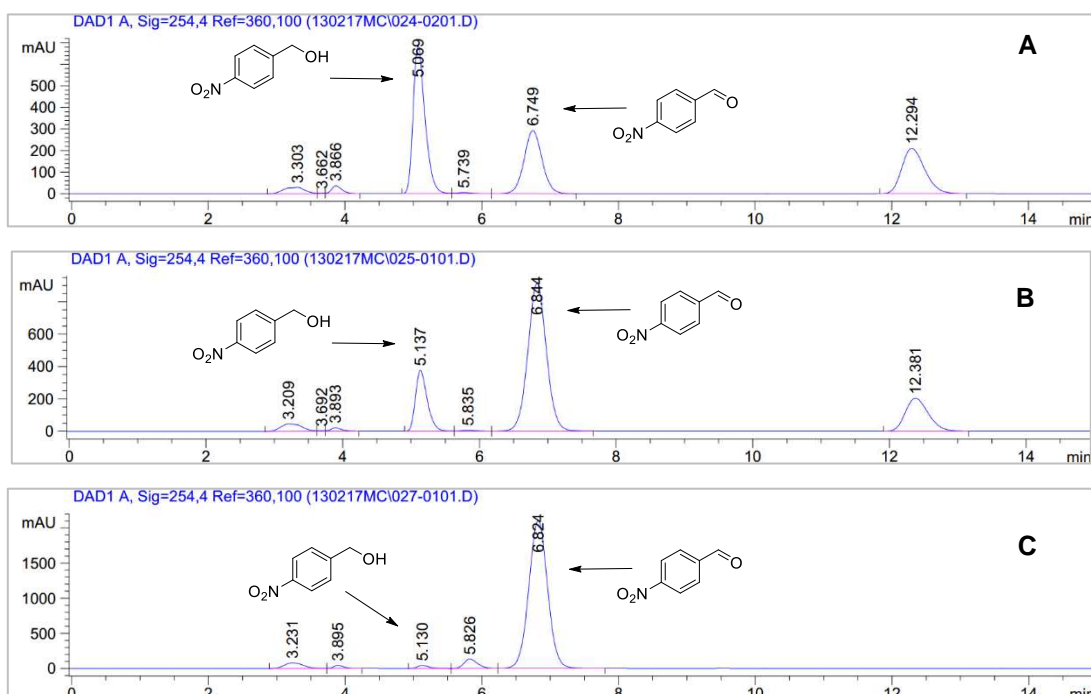


Figure S17. HPLC traces of continuous-flow oxidation of 4-nitrobenzyl alcohol, using GOase M₃₋₅ biocatalyst. Traces indicate solution composition after 1 RV (**A**), 3 RVs (**B**) and at steady-state (**C**). Peak observed at ~ 5.7 minutes attributable to a UV-active substance derived from commercially obtained 4-nitrobenzyl alcohol.

4-(Trifluoromethyl)benzaldehyde, 2e:

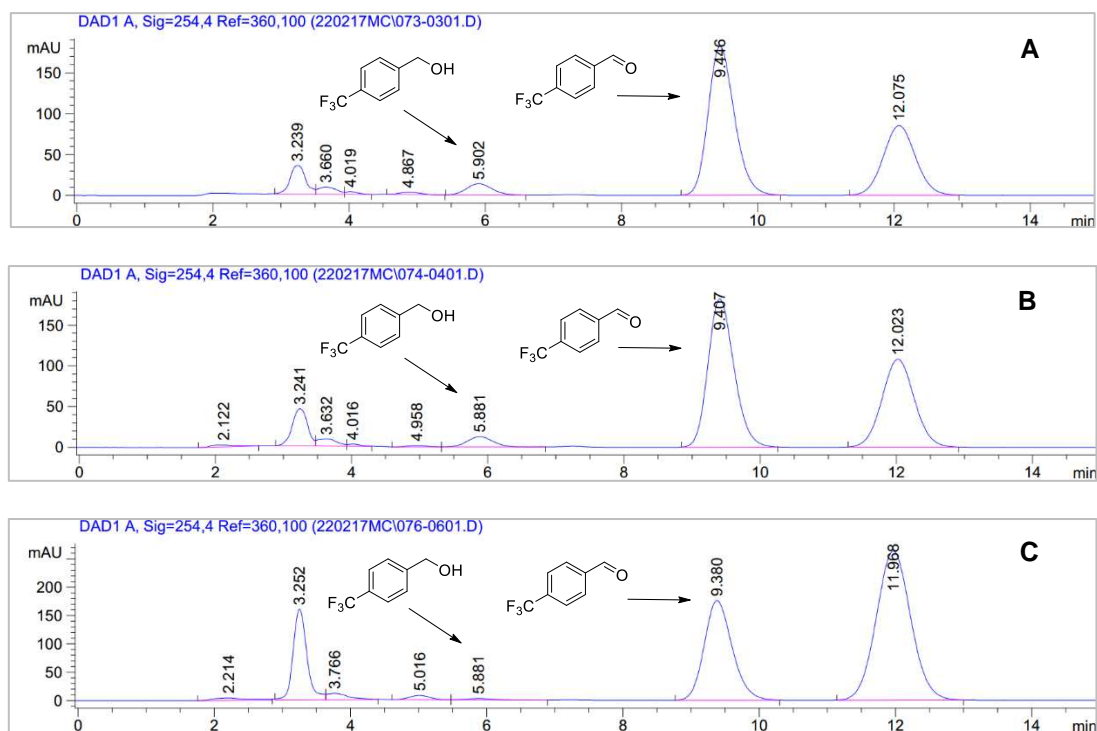


Figure S18. HPLC traces of continuous-flow oxidation of 4-(trifluoromethyl)benzyl alcohol, using GOase M_{3.5} biocatalyst. Traces indicate solution composition after 1 RV (A), 3 RVs (B) and at steady-state (C). Peak observed at ~ 4.8 minutes attributable to a UV-active substance derived from commercially obtained 4-(trifluoromethyl)benzyl alcohol.

4-(t-Butyl)benzaldehyde, 2f:

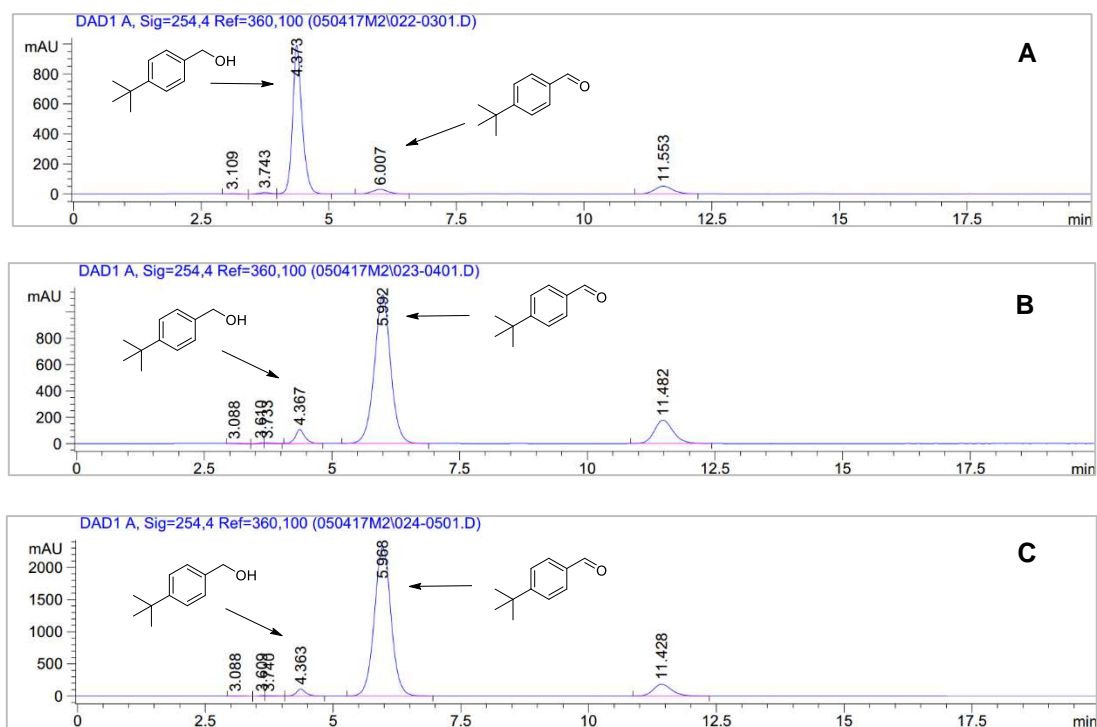


Figure S19. HPLC traces of continuous-flow oxidation of 4-(t-butyl)benzyl alcohol, using GOase M_{3.5} biocatalyst. Traces indicate solution composition after 1 RV (A), 3 RVs (B) and at steady-state (C).

3-Fluorobenzaldehyde, 2g:

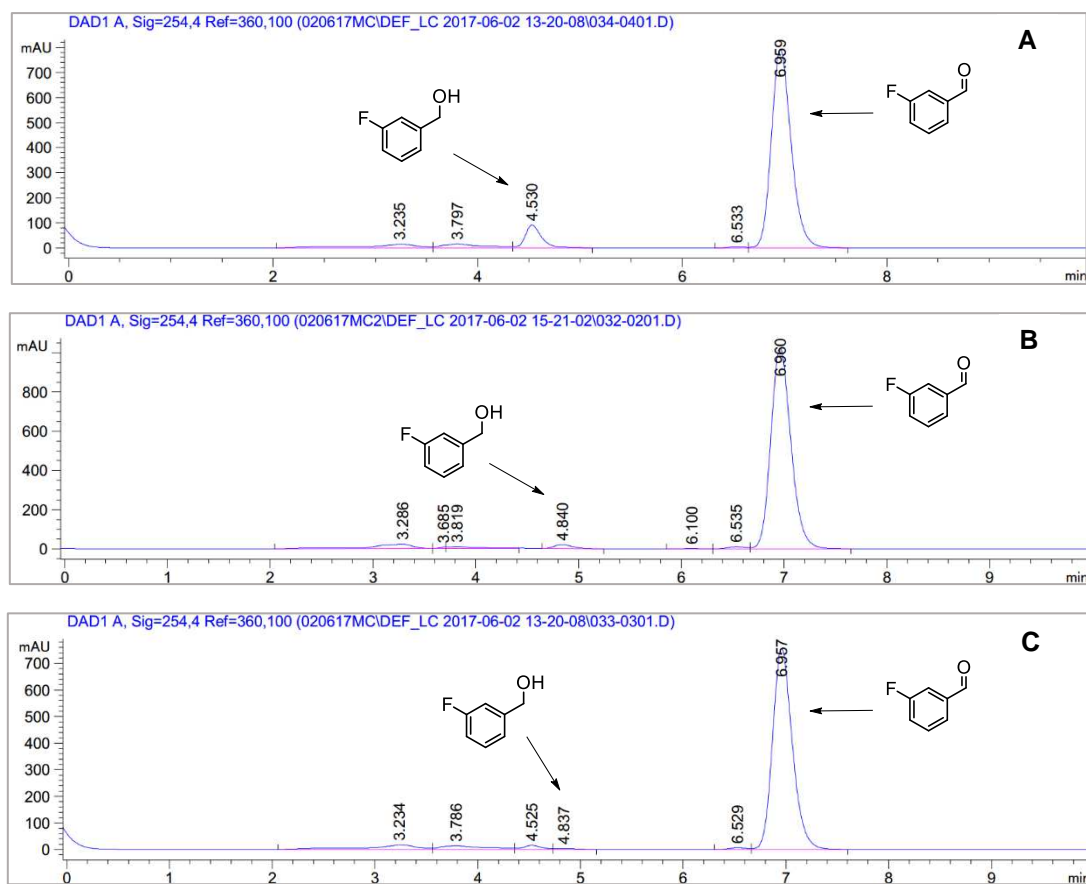
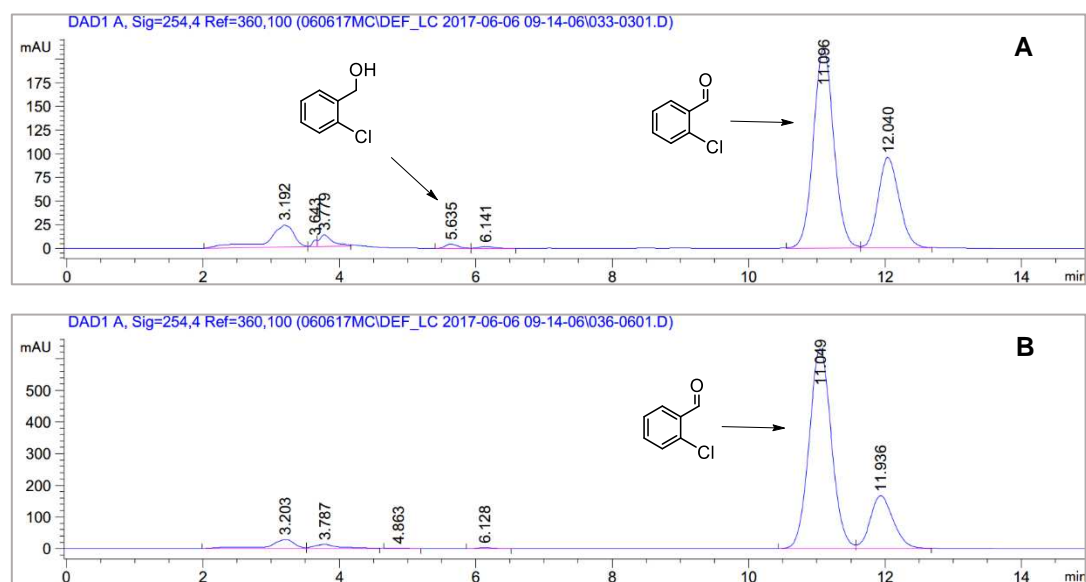


Figure S20. HPLC traces of continuous-flow oxidation of 3-fluorobenzyl alcohol, using GOase M₃₋₅ biocatalyst. Traces indicate solution composition after 1 RV (**A**), 3 RVs (**B**) and at steady-state (**C**).

2-Chlorobenzaldehyde, 2h:



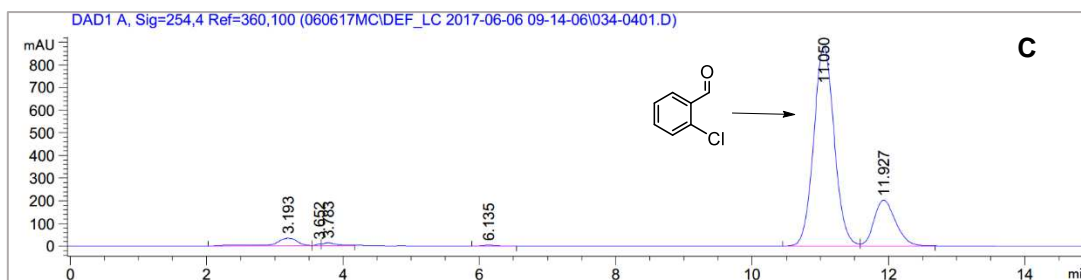


Figure S21. HPLC traces of continuous-flow oxidation of 2-chlorobenzyl alcohol, using GOase M_{3,5} biocatalyst. Traces indicate solution composition after 1 RV (A), 3 RVs (B) and at steady-state (C).

4-Bromobenzaldehyde, 2i:

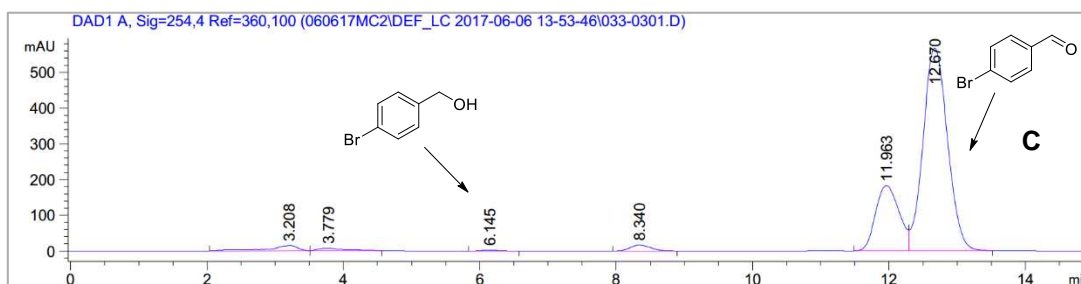
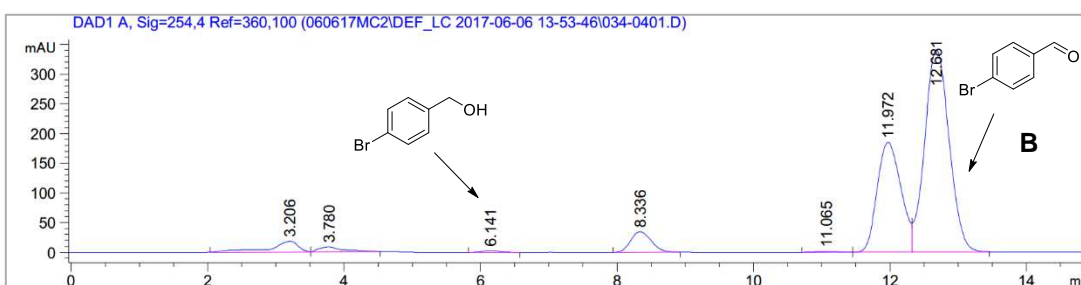
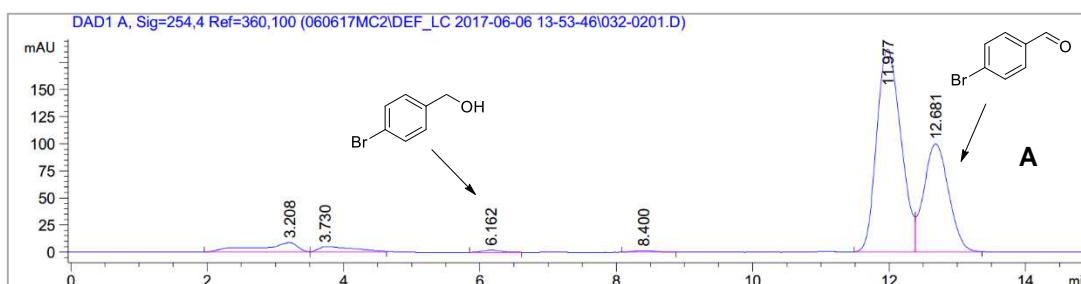
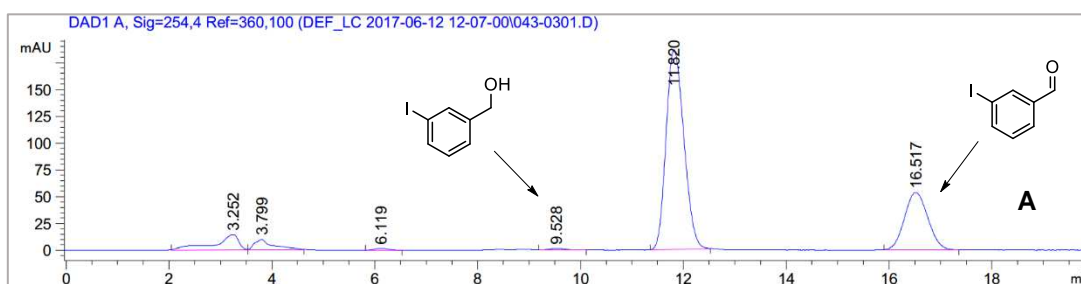


Figure S22. HPLC traces of continuous-flow oxidation of 4-bromobenzyl alcohol, using GOase M_{3,5} biocatalyst. Traces indicate solution composition after 1 RV (A), 3 RVs (B) and at steady-state (C).

3-Iodobenzaldehyde, 2j:



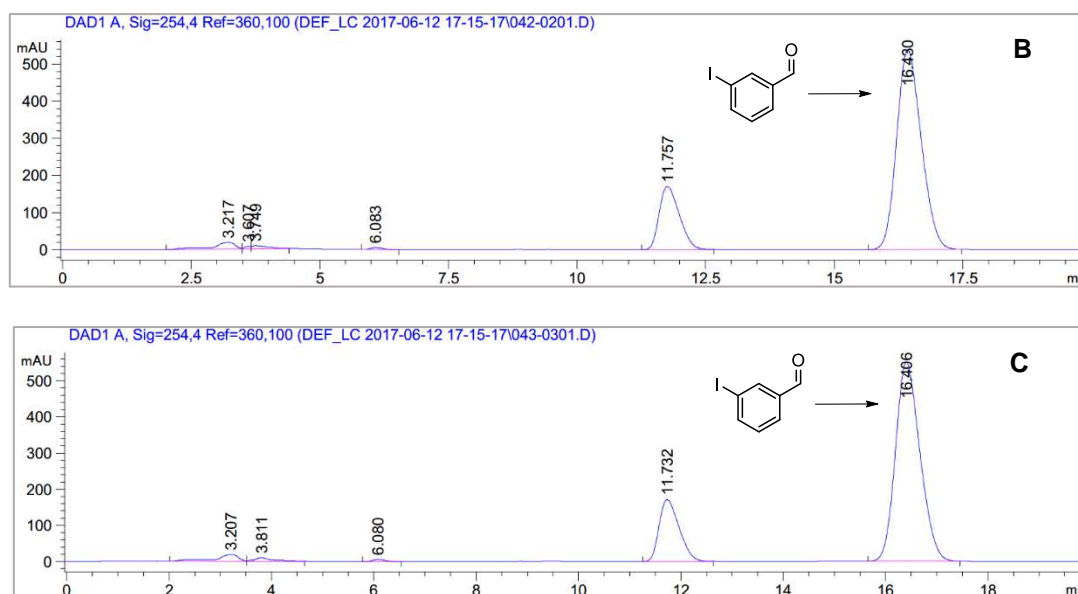


Figure S23. HPLC traces of continuous-flow oxidation of 3-iodobenzyl alcohol, using GOase M₃₋₅ biocatalyst. Traces indicate solution composition after 1 RV (A), 3 RVs (B) and at steady-state (C).

4-(Thiomethyl)benzaldehyde, 2k:

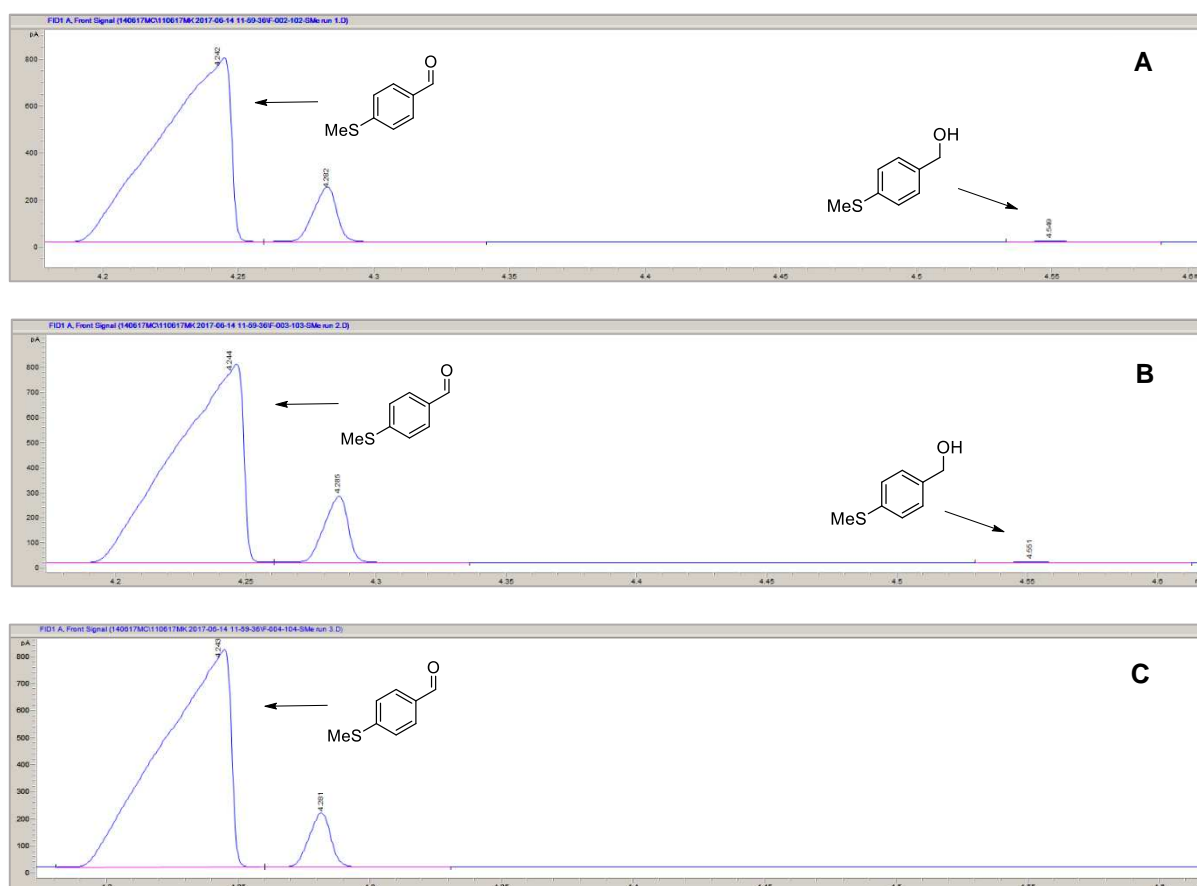


Figure S24. GC traces of continuous-flow oxidation of 4-(thiomethyl)benzyl alcohol, using GOase M₃₋₅ biocatalyst. Traces indicate solution composition after 1 RV (A), 3 RVs (B) and at steady-state (C). Peak shown at 4.28 minutes = ISTD.

3,5-Dimethoxybenzaldehyde, 2l:

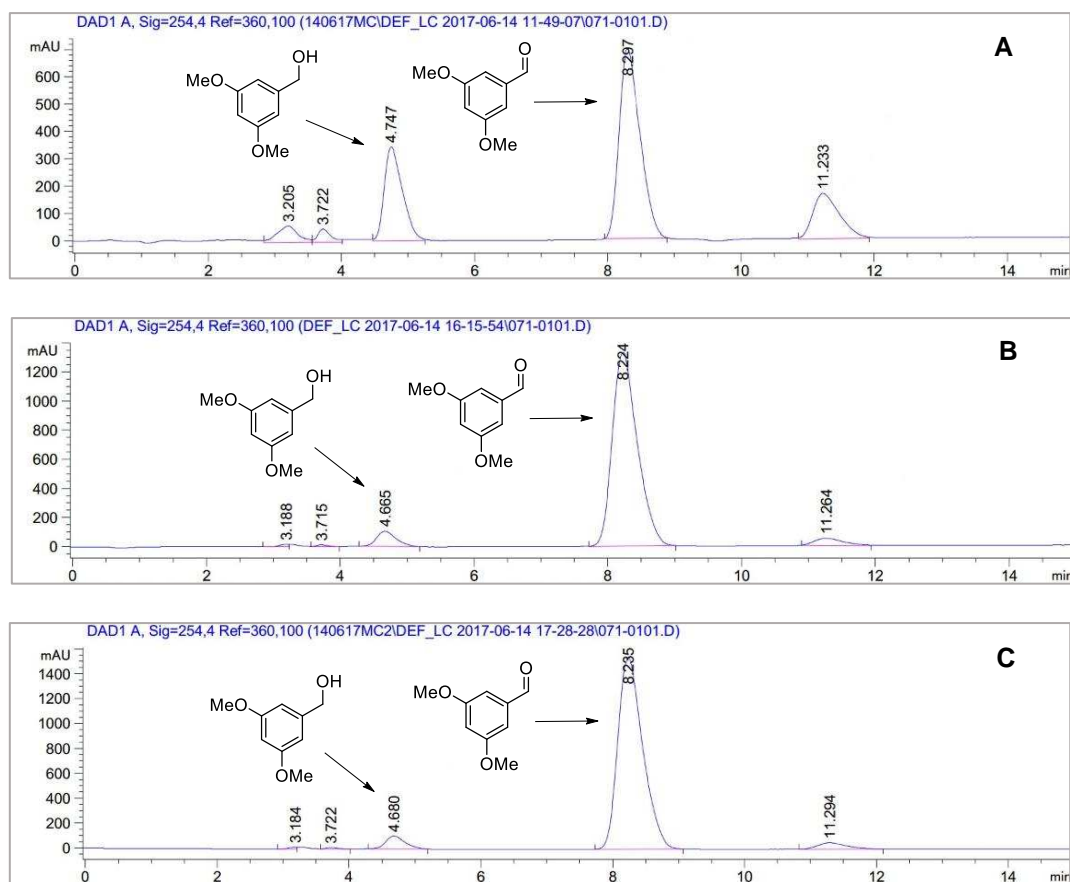
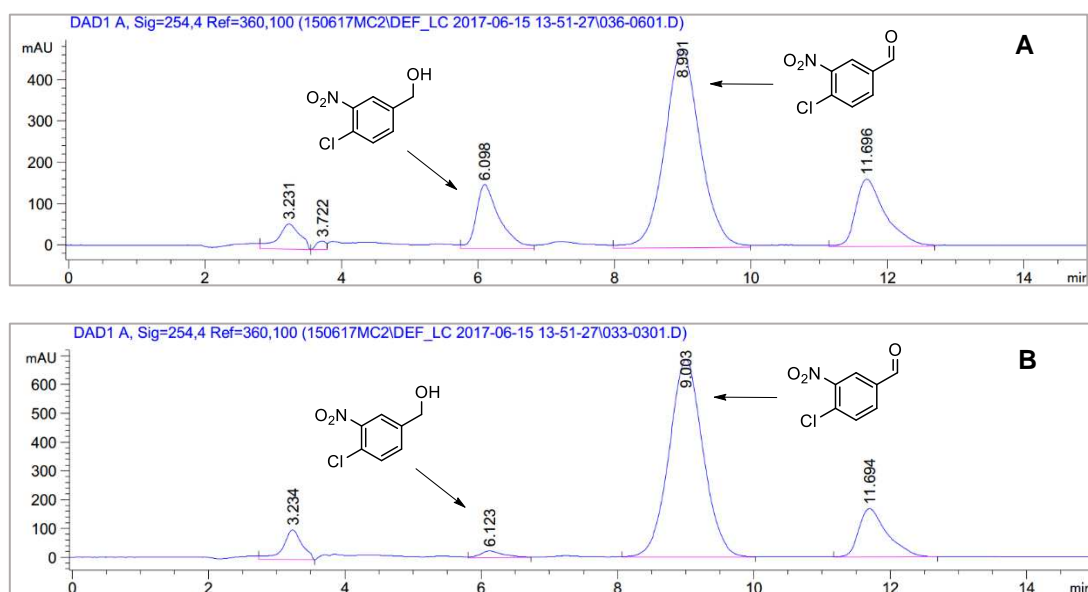


Figure S25. HPLC traces of continuous-flow oxidation of 3,5-dimethoxybenzyl alcohol, using GOase M_{3,5} biocatalyst. Traces indicate solution composition after 1 RV (**A**), 3 RVs (**B**) and at steady-state (**C**).

3-Nitro-4-chlorobenzaldehyde, 2m:



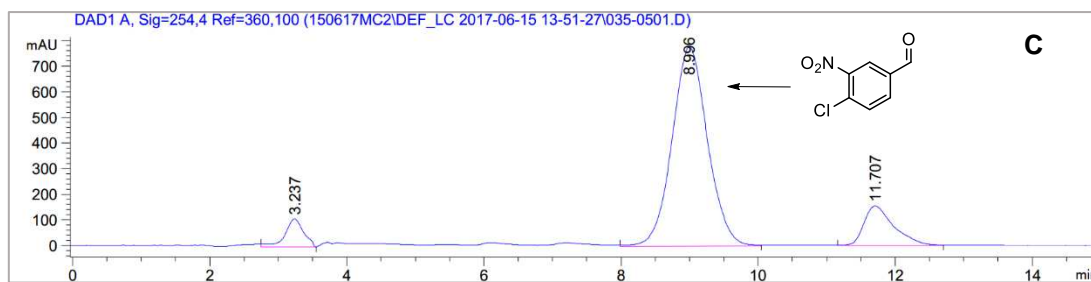


Figure S26. HPLC traces of continuous-flow oxidation of 3-nitro-4-chlorobenzyl alcohol, using GOase M₃₋₅ biocatalyst. Traces indicate solution composition after 1 RV (A), 3 RVs (B) and at steady-state (C).

2-Pyridinecarboxaldehyde, 2n:

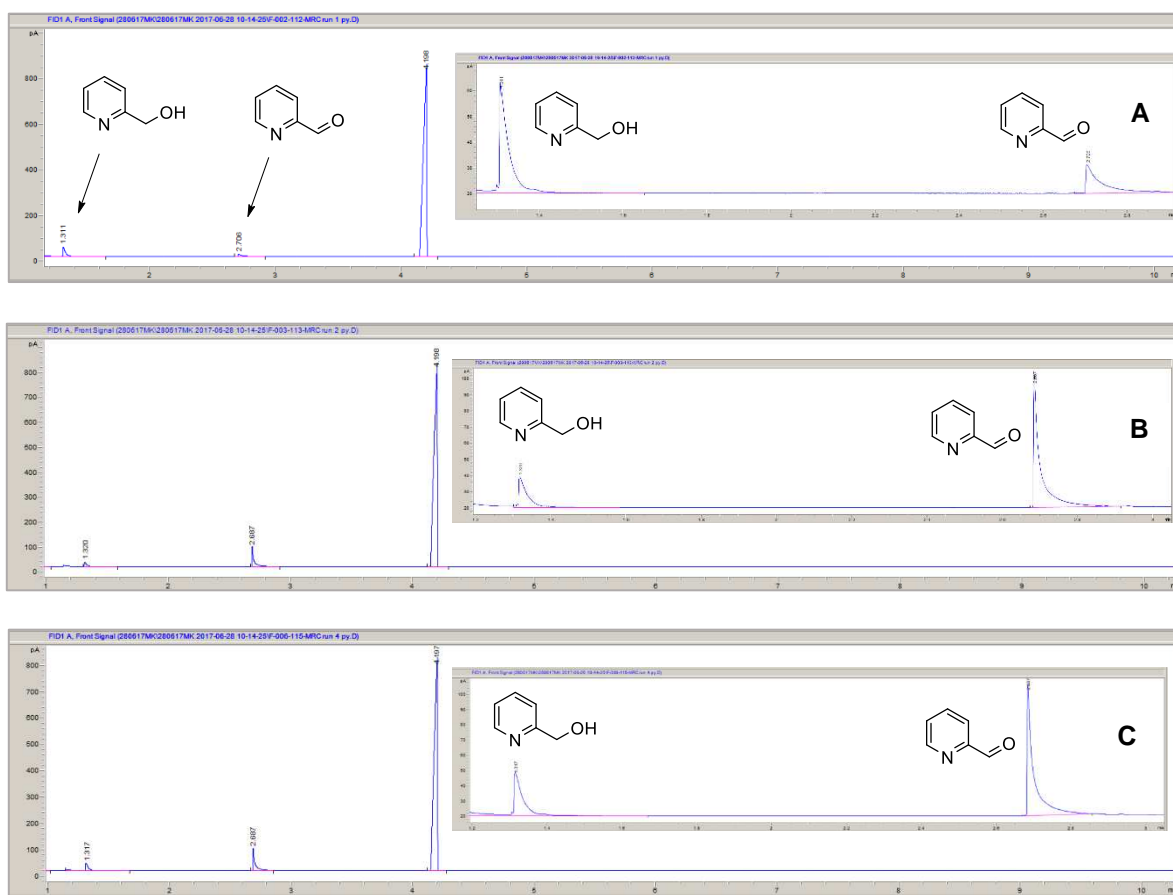


Figure S27. GC traces of continuous-flow oxidation of 2-pyridinemethanol, using GOase M₃₋₅ biocatalyst. Traces indicate solution composition after 1 RV (A), 3 RVs (B) and at steady-state (C). Peak shown at 4.20 minutes = ISTD.

2-Thiophenecarboxaldehyde, 2o:



Figure S28. GC traces of continuous-flow oxidation of 2-thiophenemethanol, using GOase M₃₋₅ biocatalyst. Traces indicate solution composition after 1 RV (A), 3 RVs (B) and at steady-state (C). Peak shown at 4.20 minutes = ISTD.

2,5-Diformylfuran, 2p:



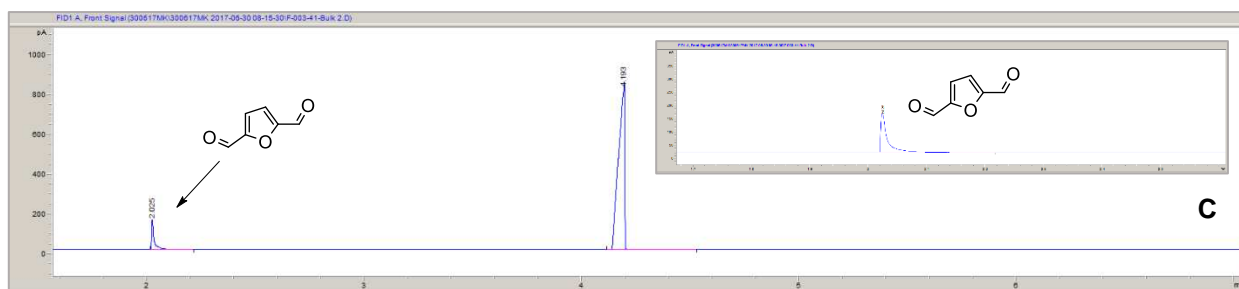


Figure S29. GC traces of continuous-flow oxidation of 5-hydroxymethylfurfural, using GOase M_{3.5} biocatalyst. Traces indicate solution composition after 1 RV (A), 3 RVs (B) and at steady-state (C). Peak shown at 4.20 minutes = ISTD.

3,4-Dihydroisoquinoline, 4a:

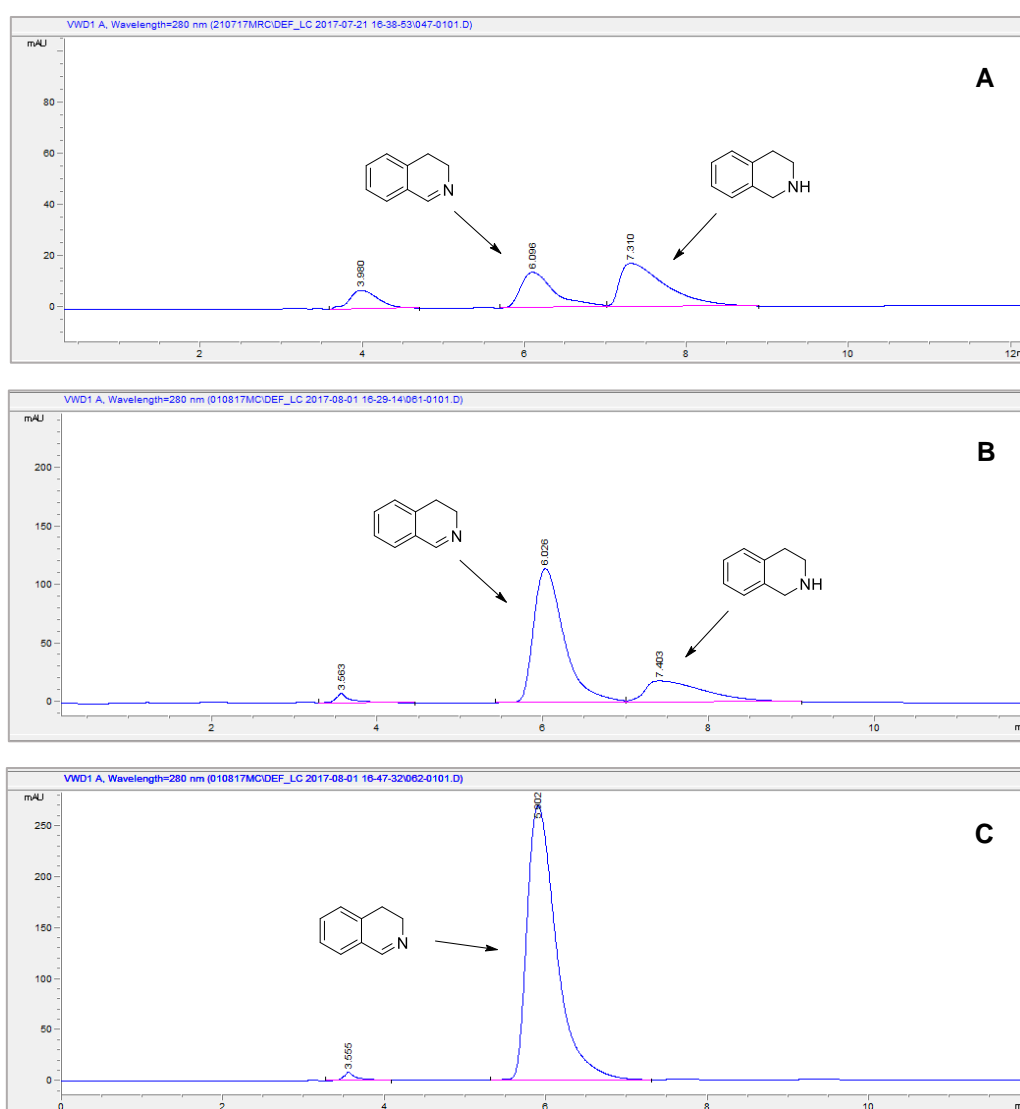


Figure S30. HPLC traces of continuous-flow oxidation of THIQ, using MAO D9 biocatalyst. Traces indicate solution composition after 1 RV (A), 3 RVs (B) and at steady-state (C). Peak shown at 3.5 minutes = AF-204.

9. HPLC Columns, Conditions and Retention Times

Achiral HPLC analysis was performed on an Agilent Technologies 1100 series system, using a YMC-pack ODS-AM, AM303 column (250 mm × 4.6 mm × 5 μm). Measurements were carried out at T = 30 °C, flow-rate = 1 mLmin⁻¹, λ = 254 nm. The identities of compounds were confirmed by comparison with independently synthesised samples where necessary.

Substrate	Product	H ₂ O:MeCN running solvent ratio ^a	Substrate R _t (min)	Product R _t (min)
1a	2a	70:30	4.76	6.76
1b	2b	70:30	4.66	6.87
1c	2c	70:30	4.45	5.72
1d	2d	70:30	5.13	6.84
1e	2e	50:50	5.88	9.40
1f	2f	35:65	4.36	5.99
1g	2g	60:40	4.84	6.96
1h	2h	60:40	5.64	11.05
1i	2i	70:30	6.14	12.68
1j	2j	60:40	9.53	16.43
1l	2l	60:40	4.68	8.23
1m	2m	60:40	6.12	9.00

Table S11. Achiral HPLC conditions and compound retention times. ^aAll solvents incorporated 0.1% TFA.

9.1 HPLC sampling

HPLC samples were prepared as follows: an aliquot of the reactor eluent (0.6 mL) was removed and aqueous NaOH (10 M, 50 μL) added followed by dichloromethane (1 mL), and the sample vigorously mixed by means of a vortex mixer. The sample was centrifuged at 10000 × g for 5 minutes, and the organic layer separated, dried over MgSO₄ and analysed by HPLC.

10. GC Columns, Conditions and Retention Times

Achiral GC analysis was performed on an Agilent Technologies 7890B series system, using a HP-1 column (30 m × 0.32 mm × 0.25 μm). The identities of compounds were confirmed by comparison with independently synthesised samples where necessary.

Substrate	Product	Substrate R _t (min)	Product R _t (min)
1k	2k	4.55	4.24
1n	2n	1.31	2.71
1o	2o	1.30	1.53
1p	2p	3.14	2.00

Table S12. GC conditions and compound retention times. ^aAll solvents incorporated 0.05% DEA.

11. References

- [1] A. Toftgaard Pedersen, W. R. Birmingham, G. Rehn, S. J. Charnock, N. J. Turner, J. M. Woodley, Org. Process Res. Dev. **2015**, 19, 1580–1589.